Lappeenranta
University of Technology

Samuli Kallio

MODELING AND PARAMETER ESTIMATION OF DOUBLE-STAR PERMANENT MAGNET SYNCHRONOUS MACHINES

Thesis for the degree of Doctor of Science (Technology) to be presented with due permission for public examination and criticism in the Auditorium 1383 at Lappeenranta University of Technology, Lappeenranta, Finland on the 5th of March, 2014, at noon.

Acta Universitatis
Lappeenrantaensis 570

Supervisor Professor Pertti Silventoinen
Department of Electrical Engineering
LUT Institute of Energy Technology (LUT Energy)
LUT School of Technology
Lappeenranta University of Technology
Finland

Reviewers Professor Emil Levi
Department of Electric Machines and Drives
Liverpool John Moores University
Liverpool, United Kingdom

D.Sc. (Tech.) Jukka Kaukonen
ABB Oy
Finland

Opponent Professor Emil Levi
Department of Electric Machines and Drives
Liverpool John Moores University
Liverpool, United Kingdom

ISBN 978-952-265-563-9
ISBN 978-952-265-564-6 (PDF)
ISSN-L 1456-4491
ISSN 1456-4491

Lappeenrannan teknillinen yliopisto
Yliopistopaino 2014

Abstract

Lappeenranta University of Technology
Acta Universitatis Lappeenrantaensis 570

Samuli Kallio

Modeling and Parameter Estimation of Double-Star Permanent Magnet Synchronous Machines

Lappeenranta 2014
68 p.

ISBN 978-952-265-563-9
ISBN 978-952-265-564-6 (PDF)
ISSN-L 1456-4491, ISSN 1456-4491

The power rating of wind turbines is constantly increasing; however, keeping the voltage rating at the low-voltage level results in high kilo-ampere currents. An alternative for increasing the power levels without raising the voltage level is provided by multiphase machines. Multiphase machines are used for instance in ship propulsion systems, aerospace applications, electric vehicles, and in other high-power applications including wind energy conversion systems.

A machine model in an appropriate reference frame is required in order to design an efficient control for the electric drive. Modeling of multiphase machines poses a challenge because of the mutual couplings between the phases. Mutual couplings degrade the drive performance unless they are properly considered. In certain multiphase machines there is also a problem of high current harmonics, which are easily generated because of the small current path impedance of the harmonic components. However, multiphase machines provide special characteristics compared with the three-phase counterparts: Multiphase machines have a better fault tolerance, and are thus more robust. In addition, the controlled power can be divided among more inverter legs by increasing the number of phases. Moreover, the torque pulsation can be decreased and the harmonic frequency of the torque ripple increased by an appropriate multiphase configuration. By increasing the number of phases it is also possible to obtain more torque per RMS ampere for the same volume, and thus, increase the power density.

In this doctoral thesis, a decoupled d–q model of double-star permanent-magnet (PM) synchronous machines is derived based on the inductance matrix diagonalization. The double-star machine is a special type of multiphase machines. Its armature consists of two three-phase winding sets,

which are commonly displaced by 30 electrical degrees. In this study, the displacement angle between the sets is considered a parameter. The diagonalization of the inductance matrix results in a simplified model structure, in which the mutual couplings between the reference frames are eliminated. Moreover, the current harmonics are mapped into a reference frame, in which they can be easily controlled. The work also presents methods to determine the machine inductances by a finite-element analysis and by voltage-source inverters on-site.

The derived model is validated by experimental results obtained with an example double-star interior PM (IPM) synchronous machine having the sets displaced by 30 electrical degrees. The derived transformation, and consequently, the decoupled d–q machine model, are shown to model the behavior of an actual machine with an acceptable accuracy. Thus, the proposed model is suitable to be used for the model-based control design of electric drives consisting of double-star IPM synchronous machines.

Keywords: double-star, estimation, modeling, permanent-magnet synchronous machine
UDC 621.313.3:51.001.57:519.62/.64:004.94

Acknowledgments

The research documented in this doctoral thesis was carried out at Lappeenranta University of Technology (LUT) at the Institute of Energy Technology (LUT Energy) during the years 2010–2013. The research was funded partly by The Switch Drive Systems Oy.

I would like to express my gratitude to my supervisor, Prof. Pertti Silventoinen, for introducing me with this interesting research topic and guiding me through the process. I wish to thank Prof. Olli Pyrhönen and Dr. Pasi Peltoniemi for the guidance and excellent advice and ideas. You all played a significant role in the completion of this process. Mr. Jussi Karttunen deserves special thanks for many productive technical conversations. Jussi was always ready to help with great enthusiasm, and his thorough comments on the articles helped me revise them more understandable and consistent. I would also like to thank Dr. Riku Pöllänen and Mr. Tomi Knuutila from The Switch Drive Systems Oy for giving the initiative to begin researching this topic. The laboratory personnel of LUT are thanked for their help building up the experimental setup.

During the years I have also had the privilege to work with Prof. Mauro Andriollo and his colleagues at the University of Padova, Italy. Prof. Andriollo's expertise on electrical machines and guidance with the Maxwell 2-D program helped considerably in the completion of the doctoral thesis. You and your team deserve my warmest gratitude!

The comments by the preliminary examiners Prof. Emil Levi and Dr. Jukka Kaukonen are the most gratefully appreciated.

I am very grateful to Dr. Hanna Niemelä for her help in improving the language of the thesis, including the published articles.

The financial support by the Walter Ahlström Foundation, Ulla Tuominen Foundation, Finnish Foundation for Technology Promotion, and Research Foundation of Lappeenranta University of Technology was and is greatly appreciated.

Last but not least of all, I would like to express my gratitude to my wife for her encouragement and patience over the years and for tolerating my research enthusiasm that I so often have taken home with me.

Helsinki, February 2014

Samuli Kallio

Jos tiedät, mitä olet tekemässä, pidä toinen käsi taskussa.
Jos et tiedä, mitä olet tekemässä, pidä molemmat kädet taskussa.

kansanviisaus

Contents

Nomenclature

Latin alphabet

$\mathbf{a}$	phase rotation operator $\mathbf{a} = e^{\mathrm{j}2\pi/n}$
$\mathbf{E}$	electromotive force vector
$\mathbf{F}$	transformation matrix
$\mathbf{I}$	current vector
$\mathbf{J}$	coupling matrix
$\mathbf{L}$	inductance matrix
$\mathbf{M}$	mutual inductance matrix, vector
$\mathbf{R}$	resistance matrix
$\mathbf{T}$	transformation matrix
$\mathbf{U}$	voltage vector
A	amplitude
c	scaling coefficient [-]
e	electromotive force [V]
g	air-gap length [m]
I	current [A]
i	current [A]
k	order of harmonic [-], winding factor [-]
L	inductance, self-inductance [$\frac{\mathrm{Vs}}{\mathrm{A}}$]
l	effective length, stack length [m]
M	mutual inductance [$\frac{\mathrm{Vs}}{\mathrm{A}}$]
m	number of winding sets [-]
N	number of turns [-], winding function [-]
n	number of phases [-], order of harmonic [-]
p	time derivative operator, number of pole pairs [-]
R	resistance [$\frac{\mathrm{V}}{\mathrm{A}}$]
r	effective radius of the stator bore [m]
t	time [s]
U	voltage [V]
u	voltage [V]
z	number of nonflux/torque-producing reference frames [-]
j	imaginary unit

Greek alphabet

α	alpha axis, half of the displacement between two winding sets [rad]
β	beta axis

ϵ_1	auxiliary variable
ϵ_2	auxiliary variable
γ	displacement angle [rad]
κ	displacement between two winding sets [rad]
λ	permeance coefficient [-]
$\boldsymbol{\Psi}$	flux linkage vector
μ_0	vacuum permeability [$\frac{\mathrm{Vs}}{\mathrm{Am}}$], $\mu_0 \approx 4\pi 10^{-7}$ [$\frac{\mathrm{Vs}}{\mathrm{Am}}$]
ω	angular frequency [$\frac{\mathrm{rad}}{\mathrm{s}}$]
ϕ	circumferential position [rad], displacement angle [rad]
ψ	flux linkage [Vs]
θ	rotor position [rad]
δ	rotor position [rad]

Subscripts

d	direct-axis
$\mathrm{D_1}$	$\mathrm{D_1}$-axis of the decoupled model
$\mathrm{D_2}$	$\mathrm{D_2}$-axis of the decoupled model
e	electrical
f	field winding, magnetizing
max	maximum
min	minimum
PM	Permanent Magnet
q	quadrature-axis
$\mathrm{Q_1}$	$\mathrm{Q_1}$-axis of the decoupled model
$\mathrm{Q_2}$	$\mathrm{Q_2}$-axis of the decoupled model
r	rotor
s	stator
$\sigma 1$	self-leakage of three-phase winding set no. 1
$\sigma 2$	self-leakage of three-phase winding set no. 2
$\sigma \mathrm{m}$	mutual leakage
$\sigma \mathrm{s}$	self leakage
i	index
ij	between ith and jth phase
j	index
n	order of harmonic
α	alpha-axis of stationary reference frame
β	beta-axis of stationary reference frame
$\mathrm{a_1}$	phase a of three-phase winding set no. 1
$\mathrm{a_2}$	phase a of three-phase winding set no. 2
$\mathrm{b_1}$	phase b of three-phase winding set no. 1
$\mathrm{b_2}$	phase b of three-phase winding set no. 2
$\mathrm{c_1}$	phase c of three-phase winding set no. 1
$\mathrm{c_2}$	phase c of three-phase winding set no. 2
$\mathrm{d_1}$	direct-axis of three-phase winding set no. 1
$\mathrm{d_2}$	direct-axis of three-phase winding set no. 2
diag	diagonal
DQ	decoupled d–q reference frame

dq	d–q reference frame
ew	end winding
kd	direct-axis damper winding
kq	quadrature-axis damper winding
$\mathrm{m0}$	fundamental component
$\mathrm{m2}$	second-harmonic component
md	direct-axis magnetizing
mq	quadrature-axis magnetizing
m	magnetizing
$\mathrm{q_1}$	quadrature-axis of three-phase winding set no. 1
$\mathrm{q_2}$	quadrature-axis of three-phase winding set no. 2
rot	rotational
$\mathrm{s0}$	fundamental component
$\mathrm{s1}$	stator variable of three-phase winding set no. 1
$\mathrm{s2}$	stator variable of three-phase winding set no. 2, second-harmonic component
src	source
VSD	Vector Space Decomposition
$\mathrm{w1}$	winding fundamental component
x	x-axis of stationary reference frame
y	y-axis of stationary reference frame
1	three-phase winding set no. 1
12	three-phase winding sets 1 and 2
2	three-phase winding set no. 2

Other symbols

$\hat{}$	peak value
$\overline{\mathbf{c}}$	complex vector
$\overline{\mathbf{T}}$	complex transformation matrix
$\vec{f}$	complex variable

Acronyms

AC	Alternating Current
DC	Direct Current
EMF	Electromotive Force
EU	European Union
EWEA	European Wind Energy Association
FE	Finite Element
FEA	Finite Element Analysis
FEM	Finite Element Method
IPM	Interior Permanent Magnet
MRAS	Model-Reference Adaptive System
PM	Permanent Magnet
PMSG	Permanent Magnet Synchronous Generator
PMSM	Permanent Magnet Synchronous Machine
RLS	Recursive Least Squares
RMS	Root Mean Square

VSC	Voltage Source Converter
VSD	Vector Space Decomposition
VSI	Voltage Source Inverter
WECS	Wind Energy Conversion System
WTS	Wind Turbine System
WWEA	World Wind Energy Association

List of publications

Publication I
Kallio, S., Karttunen, J., Andriollo, M., Peltoniemi, P., and Silventoinen, P. (2012), "Finite Element Based Phase-Variable Model in the Analysis of Double-Star Permanent Magnet Synchronous Machines," in *International Symposium on Power Electronics, Electrical Drives, Automation and Motion, SPEEDAM 2012*, pp. 1462–1467, Sorrento, Italy.

Publication II
Kallio, S., Andriollo, M., Tortella, A., and Karttunen, J. (2013), "Decoupled d–q Model of Double-Star Interior-Permanent-Magnet Synchronous Machines," *IEEE Transactions on Industrial Electronics*, vol. 60, no. 6, pp. 2486–2494.

Publication III
Kallio, S., Karttunen, J., Peltoniemi, P., Silventoinen, P., and Pyrhönen, O. (2014), "Determination of the Inductance Parameters for the Decoupled d–q Model of Double-Star Permanent-Magnet Synchronous Machines," *IET Electric Power Applications*, forthcoming.

Publication IV
Kallio, S., Karttunen, J., Peltoniemi, P., Silventoinen, P., and Pyrhönen, O. (2014), "Online Estimation of Double-Star IPM Machine Parameters Using RLS Algorithm," *IEEE Transactions on Industrial Electronics*, forthcoming.

Chapter 1

Introduction

1.1 Motivation

Renewable energy production has been increasing its share in the total energy production. The target of the European Union (EU) is to generate at least 20 % of its energy consumption from renewable energy sources by the year 2020 (EEA, 2012). The wind turbine system (WTS) technology, which is still considered one of the most promising renewable energy technology, plays an important role in achieving the target (Blaabjerg et al., 2012). The installed wind power capacity worldwide has been doubling every three years, the capacity being over 282 GW at the end of year 2012 (WWEA, 2012). The World Wind Energy Association (WWEA) estimates that the global installed wind power capacity could be as much as 1000 GW by the year 2020 (WWEA, 2012). The European Wind Energy Association, instead, expects 230 GW of wind power capacity to supply 15–17 % of the EU's then electricity demand (EWEA, 2013). According to the WWEA (2012), all wind turbines installed globally by the end of the year 2012 contributed 580 TWh to the worldwide electricity supply representing over 3 % of the global electricity demand. Although the global share is rather small, in some countries and regions wind has become one of the largest electricity sources. For example in Denmark, wind energy covers over 30 % of the electric power consumption (Blaabjerg and Ma, 2013).

The evolution of wind turbines over the past 30 years has been tremendous. Not only has the size of the wind turbines notably increased but also the role of power electronic converters has changed substantially. Figure 1.1 illustrates the evolution. In the 1980s, the power rating of wind turbines was only hundreds of kilowatts, and the role of power electronics in the energy conversion was negligible. However, a decade ago, the largest individual wind turbine generator was already 2 MW, and a partial-scale power converter was used to control the machine (Hansen et al., 2001). Today, much larger wind turbines are being developed that adopt full-scale power converters. The full-scale power converter gives a full variable-speed-controlled wind turbine (Blaabjerg et al., 2012) thereby increasing the power captured from the wind. According to Liserre et al. (2011), a 10 MW direct-drive high-temperature superconductor generator for offshore application is being developed by an Austrian-based company WindTec. To scale the power level even higher, the Upwind European project has stated that a 20 MW wind turbine is feasible (UpWind, 2011). However, according to Blaabjerg et al. (2012), the best-seller megawatt range is still only 1–3 MW.

The voltage level of 690 V (line-to-line RMS) of the state-of-the-art generators used in multi-

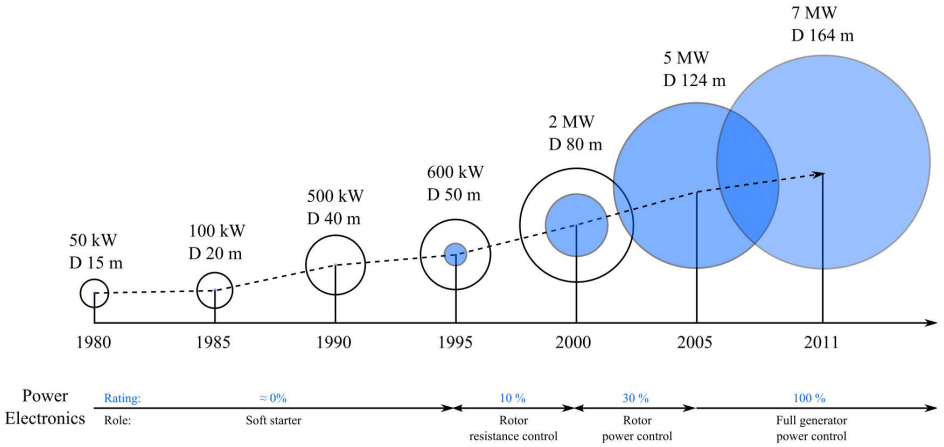

Figure 1.1: Evolution of wind turbines and the role of power electronics in the energy conversion over the last 30 years. The power level of the converters is indicated by blue. Reproduced from Blaabjerg et al. (2012).

megawatt wind energy conversion systems (WECSs) results in high (kiloamp range) stator currents. A lower phase current for the same power rating can be obtained by using multiphase generators. The multiphase generators can be connected through several low-voltage (690 V) back-to-back voltage source converters (VSCs) or diode full-bridge rectifiers into the DC link. Figure 1.2 shows an example case where a six-phase permanent-magnet (PM) generator is connected through two VSCs to the DC link and a medium-voltage grid-side converter is used for the grid connection. In this example case, the voltage of the DC link is elevated because of the series

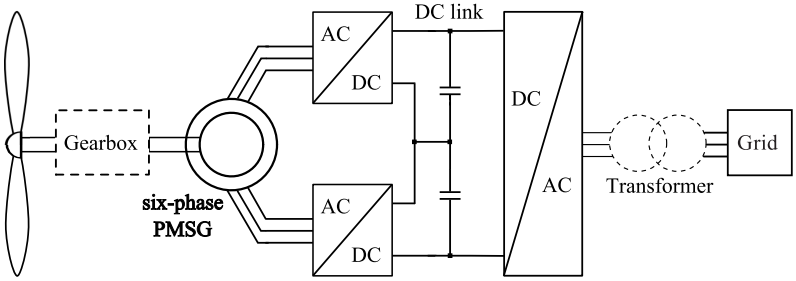

Figure 1.2: Wind energy conversion system consisting of a six-phase PM synchronous generator connected to the DC link through two VSCs arranged in series. A medium-voltage VSC connects the DC link to the grid. The gearbox and the transformer can be omitted in certain designs, and are therefore illustrated by a dashed line.

connection of the DC side of the VSCs, and thus, the operating point of the multilevel converter can be reached by keeping low-voltage at the AC terminals of the machine (Duran et al., 2011). Since the power electronics can be viewed as an interface between the grid and the generator, the number of phases of the generator is not limited to the number of phases of the grid.

In order to fully exploit the advantages such as higher reliability and better torque quality provided by multiphase machines, a simplified yet accurate machine model in an appropriate reference frame is needed. An analytical model of the machine in an appropriate reference frame is of importance especially in model-based control design; for example, in designing a predictive current control. In this study, the simplified structure serves two requirements: the electric and magnetic variables of the fundamental frequency must be represented by DC quantities and the coupling between the variables must be minimized. As the accuracy of the model depends on the machine parameters, a method for determining the model parameters is also needed.

1.2 Outline of the thesis

This doctoral thesis studies modeling and parameter estimation of double-star permanent-magnet synchronous machines. The target of this doctoral thesis is to develop an analytical model of double-star PM machines for analysis and model-based control purposes and to propose methods to determine the machine parameters. The armature of the studied machine consists of two three-phase winding sets with an arbitrary displacement angle between the sets. The rotor includes permanent magnets buried inside the rotor, thus representing a magnetically anisotropic (salient-pole) structure.

The thesis consists of four main topics:

1. Evaluation of machine-based harmonics using a phase-variable model
2. Analytical derivation of decoupled d–q reference frames for double-star PM machines
3. Determination of double-star machine parameters applying a finite element method and experimental determination by voltage source inverters
4. On-line estimation of double-star PM machine parameters using recursive least-squares algorithm

The topics are discussed in four publications.

Publication I studies how the harmonics that originate from the machine itself affect the accuracy of the analytical model of double-star permanent magnet machines. The effects are evaluated using a phase-variable model, which can take into account any number of harmonics. The parameters for the model are obtained by finite-element analyses.

Publication II derives a decoupled d–q model for double-star interior PM (IPM) machines. The derivation of the model is based on the diagonalization of the machine inductance matrix. The derived machine model is verified by experimental results using diode full-bridge rectifiers as machine-side converters.

Publication III studies the determination of the inductance parameters for the decoupled d–q model. Three methods altogether are evaluated by finite element analyses and one method by experimental results.

Publication IV proposes an on-line parameter estimation method for double-star IPM machines using the decoupled d–q model and a recursive least squares algorithm. The parameters are estimated at a standstill and in the rotating operating state. The experimental results are compared with the results obtained from the finite element analyses.

The author of this doctoral thesis is the principal author of Publications I–IV. The analytical calculations in Publication II were made in cooperation with Prof. Mauro Andriollo. In Publications I–IV the simulations were carried out by the author and the experimental tests were performed in cooperation with Mr. Jussi Karttunen. The other coauthors have participated in the commenting of the papers.

The introductory part of the thesis is divided into six chapters: Chapter 1 draws up the outline of the thesis and lists scientific contributions. Chapter 2 gives a literature review on the research topic. Chapter 3 introduces and discusses the machine parameters. Chapter 4 addresses modeling of double-star PM machines, analyzes Publication I in brief, and compares the decoupled d–q model derived in Publication II with existing methods. Chapter 5 describes Publications III and IV in brief and presents an AC standstill method in determination of inductances of double-star PM machines. Chapter 6 elaborates on the conclusions of this doctoral thesis with suggestions for future work.

1.3 Scientific contributions

The main contribution of this doctoral thesis is the derivation of an analytical model of double-star PM machines that represents the machine with two decoupled d–q reference frames. The scientific contributions of this doctoral thesis can be summarized as follows:

1. Derivation of an analytical model of double-star PM machines in decoupled d–q reference frames
2. Derivation of analytical expressions to calculate the model inductances from the phase-variable inductance waveforms
3. Determination of the parameters for the decoupled d–q model with a finite element analysis and with an experimental setup using two voltage source inverters (VSIs)
4. Estimation of the model parameters at a standstill and in the rotating operating state using two VSIs

Chapter 2

Double-star electrical machines

In general, electrical machines with more than three phases ($n > 3$) are categorized as multiphase machines (Levi et al., 2004). The armature of the machines can consist of one or more winding sets (commonly star connected). Electrical machines with multiple winding sets ($m > 1$) have magnetic couplings both between individual phases of a winding set and between the sets. There are also 'fault-tolerant' machines, which have a high degree of magnetic isolation between the phases, and because of the isolation, no cross-couplings occur (Miller and McGilp, 2009).

The history of multiphase machines dates back to the 1920s when double-winding generators were proposed to surpass the limitations on the circuit breaker interrupting capacity (Fuchs and Rosenberg, 1974). Later, multiphase machines helped to overcome the current limitations of semiconductor devices by decreasing the current per phase value (Schiferl and Ong, 1983a). Multiphase machines, which consist of two winding sets, also offered a more optimal solution to provide both AC and DC power on aircrafts and ships: DC power was supplied through a rectifier connected to one winding set while the other winding set supplied AC power. The system required less filtering but also weighed less than the conventional three-phase generator-transformer-rectifier system (Schiferl and Ong, 1983a). Double-wound synchronous machines were also used to supply AC power for air conditioners and illumination systems in DC electric railway coaches (Kataoka et al., 1981).

Multiphase machines having two three-phase stator windings spatially displaced by 30 electrical degrees have been studied in many papers from the 1970s onwards (Nelson and Krause, 1974; Fuchs and Rosenberg, 1974; Lipo, 1980; Jahns, 1980; Schiferl and Ong, 1983a; Abbas et al., 1984; Zhao and Lipo, 1995; Hadiouche et al., 2004; Bojoi et al., 2006; Andriollo et al., 2009; Barcaro et al., 2010; Tessarolo, 2010). Such machines have been called dual three-phase, dual stator-winding, or double-star machines. The terms asymmetrical six-phase and split-phase machines have also been used. The study of Nelson and Krause (1974) shows that the torque characteristic of a multiphase machine, the armature of which consists of two three-phase winding sets having a displacement of 30° between the sets, is substantially better than for 0- or 60-degree displacements. Moreover, by supplying the two three-phase sets displaced by 30° with two three-phase inverters instead of one set and one inverter, the amplitude of the pulsating torque component was reduced and the frequency was shifted to 12 times the supply frequency (Nelson and Krause, 1974). Schiferl and Ong (1983b) have also shown that for most operating conditions of a six-phase synchronous machine with AC and DC stator connections, a displacement angle of 30° appears to

be the optimum with respect to voltage harmonic distortion and torque pulsation. A further improvement in the system performance can be obtained by extending the concept to three or more inverters feeding a single machine (Nelson and Krause, 1974). Consequently, the displacement angle between the winding sets giving the best performance for n-phase machines is, in general, $180^\circ/n$ for an even number of sets and $360^\circ/n$ for an odd number of sets (Nelson and Krause, 1974). In symmetrical n-phase systems, the best performance is obtained by an angle of $360^\circ/n$ between the phases.

The main motivations to use multiphase machines instead of conventional three-phase machines relate strongly to the electric drive performance and the current rating of power converters. In the following, the main advantages of multiphase machine drives compared with conventional three-phase machine drives are listed. The statements have been gathered from (Abbas et al., 1984; Bojoi et al., 2003; Boglietti et al., 2008; Miller and McGilp, 2009)

- the controlled power can be divided among more inverter legs to reduce the current stress of single static switches instead of adopting parallel techniques,
- it is possible to smooth the torque pulsations by an appropriate choice of a winding configuration,
- the rotor harmonic losses can be reduced from the level produced in three-phase six-step systems,
- the overall system reliability is improved in case of the loss of one machine phase,
- winding factors can be increased, and
- the overall system reliability is improved in the case of the loss of one inverter module.

The feature of redundancy that multiphase machine drives also provide, especially the ones that are supplied by separate inverter units, is valuable in applications requiring at least partial power in all situations; for example, in ship propulsion systems (Kanerva et al., 2008). Thus, multiphase machines have been proposed for aerospace applications, electric vehicles, and other high-power applications requiring high reliability (Simoes and Vieira, 2002; Parsa, 2005; Levi, 2008).

Although multiphase machines have been studied rather intensively for the past three decades, little research is reported with regard to modeling of multiphase PM machines, particularly with machines with a magnetically anisotropic rotor. Moreover, it was not until the mid- to late 1990s when variable-speed multiphase drives became a serious contender for various applications (Parsa, 2005).

2.1 Modeling of double-star electrical machines

Many advantages motivate the use of transformations for the modeling of electrical machines. An important advantage is to obtain variables (fluxes, currents, and voltages) that are constants in the steady state, and are thus easier to analyze. Another advantage is the elimination of the rotor position dependency of inductances that characterizes salient pole machines – constant inductance parameters simplify the model structure, and consequently, the control of the machine. Thus, the

main issue in the modeling of electrical machines is the transformation that maps the machine variables into a proper reference frame.

Krause et al. (2002) list the reference frames commonly used in the analysis of three-phase electrical machines and power system components:

- arbitrary reference frame,
- stationary reference frame,
- reference frame fixed in the rotor, and
- synchronously rotating reference frame.

The reference frame speed defines the main difference between the four cases and requires some comments. In the arbitrary reference frame, the speed is unspecified ω. In the stationary reference frame instead, the speed is zero as the name suggests. The reference frame fixed in the rotor rotates at the rotor electrical speed ω_r, whereas the synchronously rotating reference, which rotates at the speed ω_e, rotates in synchronism with the rotating magnetic field. In the case of a synchronous machine, the latter two reference frames are exactly the same because $\omega_\mathrm{r} = \omega_\mathrm{e}$.

Air-gap space harmonics and magnetic nonlinearities complicate the use of linear analysis techniques, and therefore, some assumptions and simplifications must be made (Abbas et al., 1984). The assumptions of sinusoidally distributed windings and a linear flux path are used both for conventional three-phase machines and multiphase machines. In the case of double-star machines, also the following simplifications are generally applied (Fuchs and Rosenberg, 1974; Nelson and Krause, 1974; Abbas et al., 1984; Bojoi et al., 2003):

- The windings are equal and symmetrical within each three-phase set.
- Mutual leakage inductances are not considered.

The first simplification assumes that the parameters of the windings have the same values. The latter simplification instead assumes that the mutual leakage coupling is negligible. In general, such a coupling occurs only when coil sides of windings share the same stator slots (Schiferl and Ong, 1983a). A further simplification for the analysis can be obtained by neglecting the effect of damper windings, as in Fuchs and Rosenberg (1974). Note that the PM synchronous generators in WECSs are typically not equipped with damper windings.

The well-known Park transformation projects the stator physical phase variables to a d–q–0 reference frame fixed in the rotor (Park, 1929). The transformation matrix with a power invariant scaling to model a conventional three-phase machine in the d–q–0 reference frame is as follows:

$$\mathbf{T}_\mathrm{P}(\delta) = \sqrt{\frac{2}{3}} \begin{pmatrix} \cos\delta & \cos(\delta - \frac{2\pi}{3}) & \cos(\delta + \frac{2\pi}{3}) \\ -\sin\delta & -\sin(\delta - \frac{2\pi}{3}) & -\sin(\delta + \frac{2\pi}{3}) \\ 1/\sqrt{2} & 1/\sqrt{2} & 1/\sqrt{2} \end{pmatrix} \tag{2.1}$$

where δ defines the rotor electrical angle from its zero position. The scaling coefficient can be selected arbitrarily, but it is convenient to select it to give

- power invariant scaling $c = \sqrt{2/3}$,

- peak-value scaling $c = 2/3$, or

- RMS value scaling $c = \sqrt{2}/3$.

Assuming a sinusoidal symmetrical condition with no zero sequence component, as a result of the peak value scaling, the length of the space vector equals the peak value of the corresponding phase quantity whereas the power invariant scaling remains power invariant. The RMS value scaling, instead, yields RMS quantities, but this scaling is seldom used. Regardless of the value of the scaling factor, the application of the Park transformation to the inductance matrix of salient-pole machines eliminates the rotor position dependency of the inductances as well as represents the fundamental components with DC quantities.

The well-known Clarke transformation (Clarke, 1943), again, can be used to map the phase variables into the stationary α–β–0 reference frame. The transformation with peak-value scaling is as follows

$$\mathbf{T}_{\mathrm{C}} = \frac{2}{3}\begin{pmatrix} 1 & -\frac{1}{2} & -\frac{1}{2} \\ 0 & \frac{\sqrt{3}}{2} & -\frac{\sqrt{3}}{2} \\ \frac{1}{2} & \frac{1}{2} & \frac{1}{2} \end{pmatrix}. \tag{2.2}$$

Naturally, both the transformations (2.1) and (2.2) can be used for multiple three-phase winding sets.

Nelson and Krause (1974) have used the Park transformation to model a multiphase induction machine the armature of which consists of multiple three-phase winding sets. The transformation is applied to each of the winding sets separately. Consequently, the model is a straightforward extension of the model of three-phase machines. Similarly, Fuchs and Rosenberg (1974) have used a transformation matrix that has been constructed from two Park transformation matrices. Such a modeling method is generally known as the double d–q winding approach because of the resulting two d–q reference frames. In general, the application of the Park transformation to multiphase machines, the armature of which consists of m three-phase winding sets, results in m pairs of d–q equations (Levi, 2008). Figure 2.1 shows the double d–q reference frame equivalent circuits of double-star synchronous machines (Schiferl and Ong, 1983a) with the following parameters: R_{s} is the stator resistance, L_σ is the leakage inductance, ω_{e} is the electrical angular speed, L_{md}, and L_{mq} are the d–q axis magnetizing inductances, respectively, ψ_{d} and ψ_{q} are the d–q axis flux linkages, L_{kd} and L_{kq} are the inductances of the damper windings, R_{kd} and R_{kq} are the resistances of the damper windings, and I_{f} is the magnetizing current. The mutual leakage coupling between the stator windings, illustrated in Figure 2.1, is omitted further on.

Abbas et al. (1984) have presented the steady-state characteristics of a six-phase squirrel-cage induction motor excited by a voltage source inverter (VSI). The motor was a modified industrial three-phase machine rewound with a six-phase stator winding consisting of two three-phase winding sets displaced by 30 electrical degrees. The transformation Abbas et al. used was a symmetrical component transformation that actually originated from the transformation proposed by

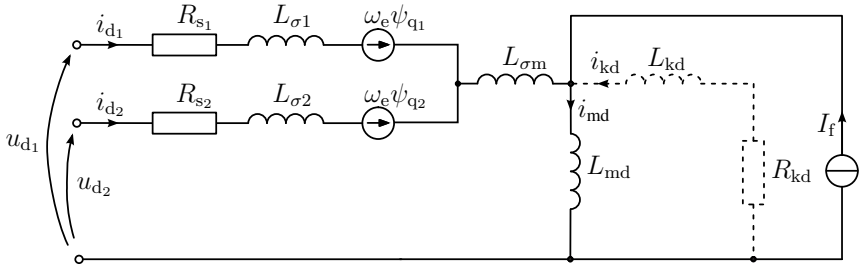

(a) d-axis

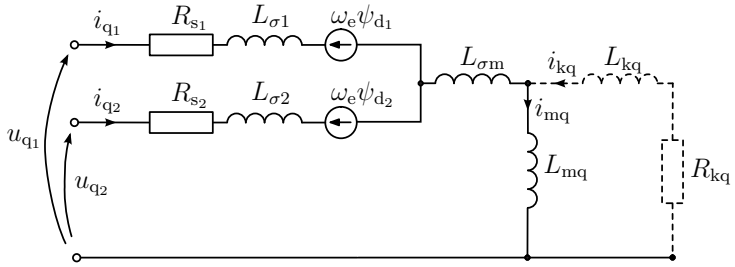

(b) q-axis

Figure 2.1: Equivalent circuits of a double-star synchronous machine when applying the Park transformation to both of the winding sets separately. The dashed lines represent the damper windings, which are neglected in this study. Adapted from Schiferl and Ong (1983a)

Fortescue (1918). The Fortescue transformation for symmetrical n-phase systems is the following:

$$\mathbf{F} = \frac{1}{\sqrt{n}} \begin{pmatrix} 1 & 1 & 1 & 1 & \cdots & 1 \\ 1 & \mathbf{a} & \mathbf{a}^2 & \mathbf{a}^3 & \cdots & \mathbf{a}^{n-1} \\ 1 & \mathbf{a}^2 & \mathbf{a}^4 & \mathbf{a}^6 & \cdots & \mathbf{a}^{2(n-1)} \\ 1 & \mathbf{a}^3 & \mathbf{a}^6 & \mathbf{a}^9 & \cdots & \mathbf{a}^{3(n-1)} \\ \vdots & \vdots & \vdots & \vdots & \cdots & \vdots \\ 1 & \mathbf{a}^{z+1} & \mathbf{a}^{2(z+1)} & \mathbf{a}^{3(z+1)} & \cdots & \mathbf{a}^{(z+1)(n-1)} \\ 1 & -1 & 1 & -1 & \cdots & -1 \\ 1 & \mathbf{a}^{z+3} & \mathbf{a}^{2(z+3)} & \mathbf{a}^{3(z+3)} & \cdots & \mathbf{a}^{(z+3)(n-1)} \\ \vdots & \vdots & \vdots & \vdots & \cdots & \vdots \\ 1 & \mathbf{a}^{n-3} & \mathbf{a}^{2(n-3)} & \mathbf{a}^{3(n-3)} & \cdots & \mathbf{a}^{(n-3)(n-1)} \\ 1 & \mathbf{a}^{n-2} & \mathbf{a}^{2(n-2)} & \mathbf{a}^{3(n-2)} & \cdots & \mathbf{a}^{(n-2)(n-1)} \\ 1 & \mathbf{a}^{n-1} & \mathbf{a}^{2(n-1)} & \mathbf{a}^{3(n-1)} & \cdots & \mathbf{a}^{(n-1)^2} \end{pmatrix} \tag{2.3}$$

where $\mathbf{a} = e^{j2\pi/n}$ and the parameter z defines the number of nonflux/torque-producing reference frames (in the case of a six-phase machine $z = 1$). In general, there are one torque-producing reference frame and one zero sequence axis if n is odd, or two zero sequence axes if n is even (Yepes et al., 2012). Since the symmetrical component transformation is appropriate only for symmetrical n-phase machines where each phase is displaced by $360/n$ electrical degrees, it cannot be directly

applied to double-star machines having a phase displacement of 30° between the winding sets. This limitation, however, can be overcome by representing the machine as a symmetrical 12 phase machine, as in Abbas et al. (1984).

For the control of double-star induction machines, Zhao and Lipo (1995) have proposed a vector space decomposition (VSD) control technique, which also separates the electromechanical and nonelectromechanical energy-conversion-related machine variables into different two-dimensional reference frames. The VSD transformation is based on finding surfaces that are orthogonal to each other and are spanned by different orders of harmonics. The transformation, applicable to double-star machines with a 30° displacement between the sets, is as follows

$$\mathbf{T} = \frac{1}{\sqrt{3}} \begin{pmatrix} 1 & \cos(\frac{2\pi}{3}) & \cos(\frac{4\pi}{3}) & \cos(\frac{\pi}{6}) & \cos(\frac{5\pi}{6}) & \cos(\frac{9\pi}{6}) \\ 0 & \sin(\frac{2\pi}{3}) & \sin(\frac{4\pi}{3}) & \sin(\frac{\pi}{6}) & \sin(\frac{5\pi}{6}) & \sin(\frac{9\pi}{6}) \\ 1 & \cos(\frac{4\pi}{3}) & \cos(\frac{2\pi}{3}) & \cos(\frac{5\pi}{6}) & \cos(\frac{\pi}{6}) & \cos(\frac{9\pi}{6}) \\ 0 & \sin(\frac{4\pi}{3}) & \sin(\frac{2\pi}{3}) & \sin(\frac{5\pi}{6}) & \sin(\frac{\pi}{6}) & \sin(\frac{9\pi}{6}) \\ 1 & 1 & 1 & 0 & 0 & 0 \\ 0 & 0 & 0 & 1 & 1 & 1 \end{pmatrix}. \tag{2.4}$$

The transformation maps the machine variables into three two-axis reference frames that are decoupled with respect to each other. Thus, the machine model and its control are simplified.

Knudsen (1995) derived an extended Park transformation matrix applicable to double-star synchronous machines having the two winding sets displaced by 30°. The extended Park transformation was a result of finding a transformation that diagonalizes the stator inductance matrix of a salient-pole double-star synchronous machine, and it is as follows (Knudsen, 1995)

$$\mathbf{T} = \frac{1}{\sqrt{2}} \begin{pmatrix} \mathbf{T}_{\mathrm{P}}(\theta) & \mathbf{T}_{\mathrm{P}}(\theta - \pi/6) \\ \mathbf{T}_{\mathrm{P}}(\theta) & -\mathbf{T}_{\mathrm{P}}(\theta - \pi/6) \end{pmatrix}. \tag{2.5}$$

Application of the extended Park transformation results in a constant inductance matrix with a minimum number of mutual couplings – similarly as the application of a conventional Park transformation to three-phase machines (Knudsen, 1995).

The objective of matrix diagonalization is to convert a square matrix into a diagonal matrix that shares the same fundamental properties of the original matrix. The entries of the diagonalized matrix are the eigenvalues of the original matrix, and the eigenvectors of the square matrix make up a new set of axes corresponding to the diagonal matrix (Tang, 2007). The main advantages of using diagonalization are reduction in the number of parameters from $n \times n$ for an arbitrary matrix to n for a diagonal matrix, yet retaining the characteristic properties of the initial matrix, and most importantly, obtaining the simplest possible form of the system.

Diagonalization of the stator inductance matrix has also been proposed by Hadiouche et al. (2000). The machine under study was a double-star induction machine with an arbitrary displacement

between the winding sets. The transformation Hadiouche et al. derived is

$$\mathbf{T} = \frac{1}{\sqrt{3}} \begin{pmatrix} 1 & \cos(\frac{2\pi}{3}) & \cos(\frac{4\pi}{3}) & \cos(\kappa) & \cos(\kappa+\frac{2\pi}{3}) & \cos(\kappa+\frac{4\pi}{3}) \\ 0 & \sin(\frac{2\pi}{3}) & \sin(\frac{4\pi}{3}) & \sin(\kappa) & \sin(\kappa+\frac{2\pi}{3}) & \sin(\kappa+\frac{4\pi}{3}) \\ 1 & \cos(\frac{4\pi}{3}) & \cos(\frac{2\pi}{3}) & \cos(\pi-\kappa) & \cos(\frac{\pi}{3}-\kappa) & \cos(\frac{5\pi}{3}-\kappa) \\ 0 & \sin(\frac{4\pi}{3}) & \sin(\frac{2\pi}{3}) & \sin(\pi-\kappa) & \sin(\frac{\pi}{3}-\kappa) & \sin(\frac{5\pi}{3}-\kappa) \\ 1 & 1 & 1 & 0 & 0 & 0 \\ 0 & 0 & 0 & 1 & 1 & 1 \end{pmatrix}, \tag{2.6}$$

where κ defines the displacement between the two winding sets. The model is constructed in a stationary reference frame, and is similar with (2.4): three two-dimensional decoupled subspaces are obtained. Moreover, different harmonics are divided into different subspaces. Later, Hadiouche et al. (2004) used the transformation to study the mutual leakage coupling in double-star induction machines with a 30° displacement between the sets.

Inductance matrix diagonalization has also been the basis of a decoupled d–q model of double-star PM machines derived by Andriollo et al. (2009). The transformation results in two d–q reference frames that are decoupled with respect to each other. The transformation can be regarded as a general transformation, since it considers the displacement angle as a parameter and does not assume a specific symmetry in the mutual inductances (the mutual inductances between the phases are considered with different coefficients). Moreover, the model takes into account the rotor-based harmonics. However, it does not take into account rotor saliency, and thus, it is not applicable to double-star PM machines with embedded magnets.

Multiphase PM machines have also been analyzed by Miller and McGilp (2009). The analysis covered six-phase and nine-phase PM machines, and the models were derived using the Park transformation. Moreover, particular attention was paid to the magnetic interactions, which are of interest in determining the performance of the machine and in designing a control system (Miller and McGilp, 2009). In addition, the mutual couplings are relevant when analyzing fault tolerance.

Figure 2.2 shows the above-mentioned transformations as milestones in the modeling of double-star machines over the past 40 years. Most of the transformations have been derived for multiphase induction machines (Nelson and Krause, 1974; Lipo, 1980; Abbas et al., 1984; Zhao and Lipo, 1995). These transformations map the machine phase variables into stationary reference frames. The transformations proposed for synchronous machines, instead, map the variables into reference frames fixed in the rotor (Knudsen, 1995; Andriollo et al., 2009). Since the stator windings of induction machines and synchronous machines are commonly similar, the transformations proposed for induction machines can be, in principle, applied to synchronous machines (and vice versa). The VSD approach proposed by Zhao and Lipo (1995) has commonly been taken in the literature when considering the modeling and control of double-star machines (Bojoi et al., 2003).

The tendency shows that the transformations result in decoupled reference frames by decomposing vector spaces or by diagonalizing the inductance matrix. All in all, decoupled two-axis reference frames have received much attention in the literature. Despite the multitude of papers considering transformations for double-star machines, it appears that no papers have discussed their applicability to double-star IPM machines, or proposed a specific transformation for double-star IPM machines. In this doctoral thesis, a transformation for double-star IPM machines is proposed.

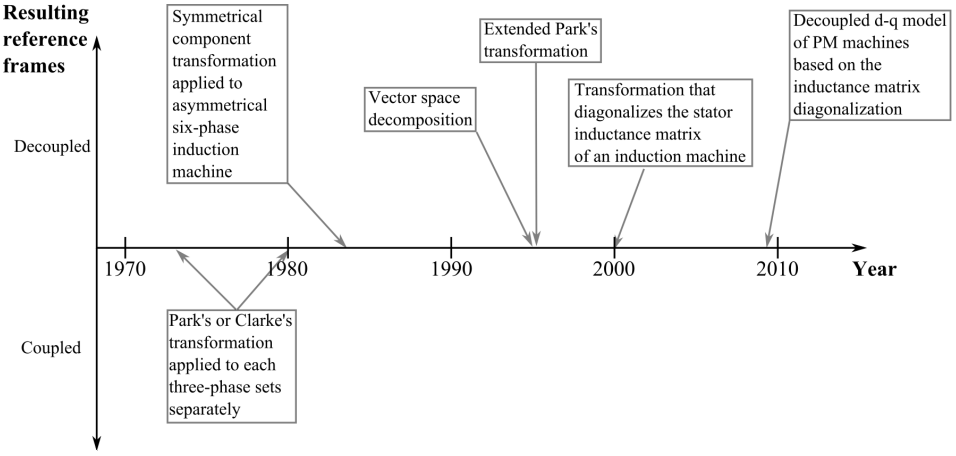

Figure 2.2: Milestones in the modeling of double-star machines from 1970 until today.

2.2 Parameter estimation of electrical machines

Machine parameter estimation methods can be divided into off-line and on-line methods. The on-line estimation methods are specified to be performed during the normal operation of the machine. The off-line methods, instead, are performed while the service of the machine is interrupted. In addition, the off-line methods include the parameter estimation of the machine using their numerical models.

The parameters of conventional three-phase IPM machines have been estimated using the d–q reference frame model and recursive least-squares (RLS)-based algorithms in Morimoto et al. (2006), Ichikawa et al. (2006), and Inoue et al. (2011). The method proposed in Ichikawa et al. (2006) also uses a signal injection and an extended EMF (electromotive force) model. Inoue et al. (2011) estimate the stator resistance on-line while the q-axis inductance is estimated off-line. Morimoto et al. (2006) instead, estimate the PM flux in the operating state and the inductance and resistance parameters are estimated at a standstill.

The state-of-the-art solutions for three-phase machines in general also include the use of an adaptive interconnected observer (Hamida et al., 2013), a converter self-commissioning at a standstill (Peretti and Zigliotto, 2012; Zubia et al., 2011), an unscented Kalman-filter-based method (Valverde et al., 2011), an extended Kalman-filter-based method (Shi et al., 2012), the use of adaptive linear neuron networks (Bechouche et al., 2012), and a multiparameter estimation (Liu et al., 2011). In addition, Liu et al. (2012) propose a model-reference adaptive system (MRAS) estimation method. The standstill methods proposed by Peretti and Zigliotto (2012) and Zubia et al. (2011) for three-phase induction machines are a step toward a complete self-commissioning of the vector-controlled drives. The nonlinear interconnected observer proposed by Hamida et al. (2013) estimates the rotor position, rotor speed, and load torque in addition to the machine parameters. The method uses the measured currents and the command voltages in the d–q reference frame. The convergence of the observer is proven by means of Lyapunov practical stability techniques.

The multiparameter on-line estimation for non-salient pole PM machines proposed by Liu et al. (2011) estimates simultaneously the winding inductance L, winding resistance R_s, and flux linkage produced by the PMs ψ_PM. The method applies an Adaline neural network and the voltage equations of the PMSM in two operating points, namely $i_\mathrm{d} = 0$ and $i_\mathrm{d} \neq 0$. Two operating points have to be considered because of the rank deficiency of the equations: if the number of estimated parameters is greater than the rank of the steady-state equations, the estimated values may not converge to the correct values, and consequently, the equation is rank deficient.

The MRAS method in Liu et al. (2012) uses the d–q model of the machine as the reference model. Liu et al. consider a surface-mounted PM machine, and thus, the reference model can be simplified further since $L_\mathrm{d} = L_\mathrm{q} = L$. Despite the simplification, the parameters L, R_s, and ψ_PM are not simultaneously identifiable because of the rank deficient problem (Liu et al., 2012). The problem can be solved by estimating first L in the $i_\mathrm{d} = 0$ condition and then estimating R_s and ψ_PM in the $i_\mathrm{d} \neq 0$ condition as done in (Liu et al., 2012).

Despite the multitude of papers on parameter estimation of three-phase machines, only a few papers consider specific estimation techniques for multiphase machines. In particular, the on-line estimation of double-star IPM machine parameters is a subject that has not been covered in the literature. Yepes et al. (2012) and Riveros et al. (2012) have recently made an effort to fill this gap by proposing parameter estimation schemes for multiphase induction machines. The methods proposed by Yepes et al. (2012) are off-line methods and do not consider on-line estimation in the rotating operating state. In Riveros et al. (2012), the parameters are estimated at a standstill using time-domain tests and the RLS algorithm. The method requires modification in the winding connection, and therefore, the method is not the most straightforward one to apply to machines on-site. In this thesis, methods to estimate double-star IPM machine parameters off-line and on-line are presented.

2.3 Conclusion

Modeling of double-star machines in general has followed two different paths: The earlier path suggests a double d–q winding approach that represents the machine with two d–q reference frames which correspond individually to the three-phase winding sets. Thus, the double d–q winding approach represents the machine with mutually coupled reference frames. The later path, a vector space decomposition approach, represents the machine with two pairs of two-axis windings (reference frames) that are orthogonal with respect to each others, and thus the coupling between the reference frames is eliminated.

Despite the multitude of papers considering transformations for double-star machines, it appears that no papers have discussed their applicability to double-star IPM machines, or proposed a specific transformation for double-star IPM machines.

Chapter 3

Parameters of double-star PM machines

This chapter introduces and discusses the equations of the main parameters needed in the modeling of double-star PM machines.

3.1 Self- and mutual inductances

Stator inductances are important in the modeling of electrical machines in general since all the stator flux linkages are related to all the stator currents through inductances. The inductances consist of self- and mutual inductances, which can be further divided into magnetizing and leakage components.

In a magnetically linear system, the self-inductance L of a winding is the ratio of the flux ψ linked by a winding to the current I flowing in the winding with all the other winding currents zero (Krause et al., 2002). For example, the self-inductance of a winding i can be expressed as follows

$$L_i = \frac{\psi_i}{I_i}. \tag{3.1}$$

Similarly, the mutual inductance linking the windings i and j results in the following expression

$$M_{ij} = \frac{\psi_j}{I_i}. \tag{3.2}$$

PM machines with buried magnets correspond to salient pole machines, in which the inductances depend on the rotor position. In such machines the fundamental wave of the self-inductance of a stator winding varies by $2\theta_\mathrm{e}$ (Vas, 1998). The dependency can be taken into account in the analytical expression of inductances with an inverse air-gap function. Krause et al. (2002) express the inverse air-gap function with the following approximation

$$g(\phi_\mathrm{s} - \theta_\mathrm{e})^{-1} = \epsilon_1 - \epsilon_2 \cos(2\phi_\mathrm{s} - 2\theta_\mathrm{e}) \tag{3.3}$$

where ϕ_s is the stator circumferential position and θ_e is the rotor position. The variables ϵ_1 and ϵ_2, defined with the help of the minimum and maximum air-gap lengths g_min and g_max, respectively,

are

$$\epsilon_1 = \frac{1}{2}\left(\frac{1}{g_{\min}} + \frac{1}{g_{\max}}\right) \tag{3.4}$$

$$\epsilon_2 = \frac{1}{2}\left(\frac{1}{g_{\min}} - \frac{1}{g_{\max}}\right). \tag{3.5}$$

This approach provides accurate results if the air gap is very small (Figueroa et al., 2006). However, it provides some insight into the influence of the machine structure in the inductances. Figure 3.1 illustrates the inverse air-gap function. For surface-mounted PM (non-salient pole) synchronous machines the effective air-gap length is approximately constant.

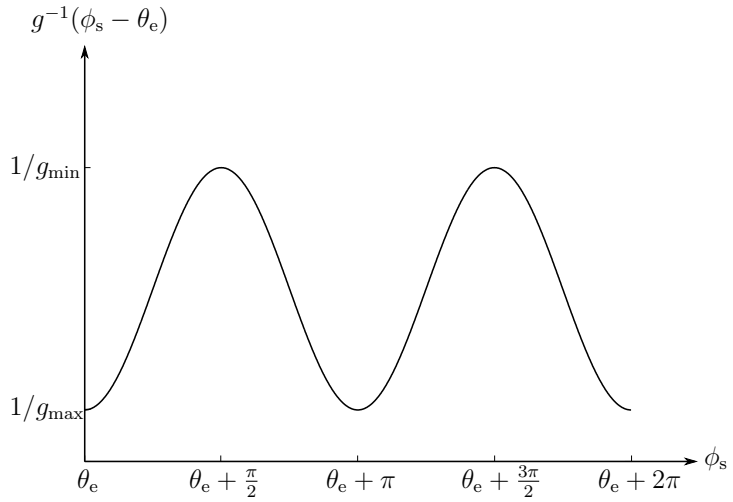

Figure 3.1: Inverse air-gap function of a sinusoidally distributed air gap.

With the help of the inverse air-gap function (3.3) and a function called the winding function $N_i(\phi_s)$, the analytical expression for the self-inductance of the stator winding i results in

$$L_i = \mu_0 r l \int_0^{2\pi} N_i(\phi_s)^2 g(\phi_s - \theta_e)^{-1} \mathrm{d}\phi_s, \tag{3.6}$$

where l is the stack length, r is the effective radius of the stator bore, and μ_0 is the permeability of vacuum ($4\pi 10^{-7}$ [Vs/Am]) (Obe, 2009). The mutual inductance linking any two stator windings i and j can be expressed similarly

$$M_{ij} = \mu_0 r l \int_0^{2\pi} N_i(\phi_s) N_j(\phi_s) g(\phi_s - \theta_e)^{-1} \mathrm{d}\phi_s. \tag{3.7}$$

These equations give the magnetizing inductances, and can be used to define all the self- and mutual inductances of the stator windings (Lipo, 2012).

Figure 3.2 shows the winding arrangement of the studied double-star PM machine. The reference

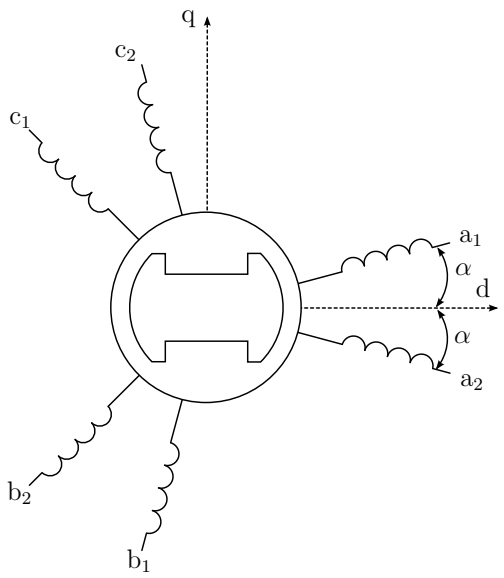

Figure 3.2: Winding arrangement of the studied double-star machine PM machine. The displacement angle α is defined in the bisection of the phases a_1 and a_2. The neutral points of the two winding sets are galvanically isolated from each other.

axis being defined in the bisection of the coils a_1 and a_2, the mathematical expression for the self-inductance of the stator winding a_1 results in

$$L_{\mathrm{a}_1}(\theta_\mathrm{e}) = L_{\mathrm{s}0} + L_{\mathrm{s}2}\cos(2\theta_\mathrm{e} + 2\alpha), \tag{3.8}$$

where $L_{\mathrm{s}2}$ is the magnetizing inductance produced by the rotor position dependent air-gap flux and $L_{\mathrm{s}0}$ consists of the magnetizing inductance caused by the fundamental air-gap flux and of the leakage inductance $L_{\sigma\mathrm{s}}$. The general expression for the self-inductance is as follows:

$$L_i(\theta_\mathrm{e}) = L_{\mathrm{s}0} + L_{\mathrm{s}2}\cos(2\theta_i), \tag{3.9}$$

where θ_i is the displacement angle from the d-axis. The higher-order harmonics of the inductances are omitted, although they may not be negligible as Publication I demonstrates. In the phase-variable model described in Publication I, the self-inductances are defined with the following equation taking into account also higher-order harmonics

$$L_i(\theta_\mathrm{e}) = L_{i\mathrm{s}0} + \sum_{n=1}^{\infty} L_{i\mathrm{s}2n}\cos(2n\theta_i + \gamma_{in}), \tag{3.10}$$

where γ_{in} is the offset of the displacement of the corresponding harmonic order n.

Mutual inductance can be defined as the ratio of the flux linked by one winding caused by the current flowing in another winding with all the other winding currents zero, as (3.2) shows. The value of the mutual inductance depends on several factors: the distance between circuits, the number of turns in each circuit, and the orientation of circuits. The shapes and sizes of circuits

also have an effect on the mutual coupling. If the winding axes are perpendicular, no mutual couplings exist. However, because of the rotor saliency, there is a rotor position dependent mutual inductance term also between perpendicular windings. For example, in double-star machines with a displacement of 30 electrical degrees between the two winding sets, the phase pairs a_1–c_2, b_1–a_2, and c_1–b_2 are perpendicular, giving a zero average value for the mutual inductance, but the rotor position dependent term, instead, is not zero. Figure 3.3 illustrates the mutual couplings related to the coil a_1 in the cases of three-phase and double-star machines. The mutual inductance between

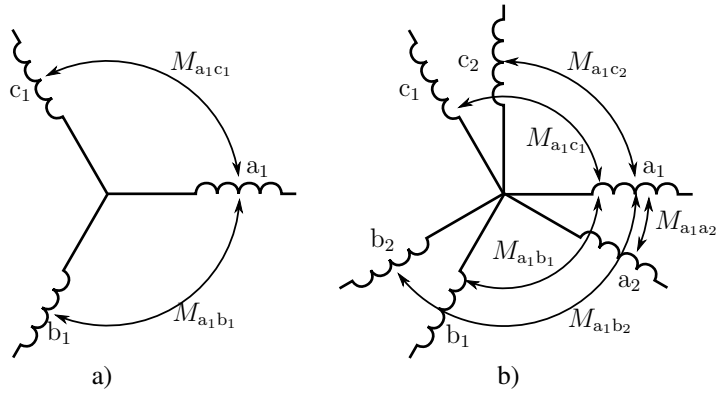

Figure 3.3: Mutual inductances related to the coil a_1 of a) a three-phase machine and b) a double-star machine.

the stator windings i and j of the same winding set can be expressed as

$$M_{ij}(\theta_\mathrm{e}) = M_{\mathrm{s}0} + M_{\mathrm{s}2}\cos(\theta_i + \theta_j). \tag{3.11}$$

where $M_{\mathrm{s}0}$ is the constant part, $M_{\mathrm{s}2}$ is the coefficient of the rotor position dependent part, and angles θ_i and θ_j define the displacement of the corresponding winding from the d-axis.

In Publication II, the mutual inductances between the coils of different winding sets are assumed with a specific symmetry, and are thus expressed as

$$M_{ij}(\theta_\mathrm{e}) = M_{\mathrm{m}0}\cos(\theta_i - \theta_j) + M_{\mathrm{m}2}\cos(\gamma_{ij}) \tag{3.12}$$

where $M_{\mathrm{m}0}\cos(\theta_i - \theta_j)$ defines the average value, $M_{\mathrm{m}2}$ is the second-harmonic coefficient, and the displacement angle γ_{ij} is defined as

$$\gamma_{ij} = \begin{cases} 2(\theta_i - \alpha) & \text{if } ij = \mathrm{a_1a_2},\ \mathrm{b_1b_2},\ \text{or } \mathrm{c_1c_2} \\ 2(\theta_i - \alpha - \pi/3) & \text{if } ij = \mathrm{a_1b_2},\ \mathrm{b_1c_2},\ \text{or } \mathrm{c_1a_2} \\ 2(\theta_i - \alpha - \pi/6) & \text{if } ij = \mathrm{a_1c_2},\ \mathrm{b_1a_2},\ \text{or } \mathrm{c_1b_2}. \end{cases} \tag{3.13}$$

Consequently, two inductance coefficients $M_{\mathrm{m}0}$ and $M_{\mathrm{m}2}$ need to be determined. The symmetric structure has been a common assumption used in the literature (Schiferl and Ong, 1983a). Publication I, instead, defines all the mutual inductances with the following general equation that can

also take into account higher-order harmonics

$$M_{ij}(\theta_\mathrm{e}) = M_{ijs0} + \sum_{n=1}^{\infty} M_{ijs2n} \cos(n(\theta_i + \theta_j) + \gamma_{in}). \tag{3.14}$$

The inductance matrix considering the stator section of double-star machines can finally be expressed as follows:

$$\mathbf{L}(\theta_\mathrm{e}) = \begin{pmatrix} \mathbf{L}_1(\theta_\mathrm{e}) & \mathbf{M}_{12}(\theta_\mathrm{e}) \\ \mathbf{M}_{21}(\theta_\mathrm{e}) & \mathbf{L}_2(\theta_\mathrm{e}) \end{pmatrix} \tag{3.15}$$

where the submatrices are given by $\left[\mathbf{M}_{21}(\theta_\mathrm{e}) = \mathbf{M}_{12}^\mathrm{T}(\theta_\mathrm{e})\right]$

$$\begin{aligned}
\mathbf{L}_1(\theta_\mathrm{e}) &= \begin{pmatrix} L_{\mathrm{a}_1}(\theta_\mathrm{e}) & M_{\mathrm{a}_1\mathrm{b}_1}(\theta_\mathrm{e}) & M_{\mathrm{a}_1\mathrm{c}_1}(\theta_\mathrm{e}) \\ M_{\mathrm{b}_1\mathrm{a}_1}(\theta_\mathrm{e}) & L_{\mathrm{b}_1}(\theta_\mathrm{e}) & M_{\mathrm{b}_1\mathrm{c}_1}(\theta_\mathrm{e}) \\ M_{\mathrm{c}_1\mathrm{a}_1}(\theta_\mathrm{e}) & M_{\mathrm{c}_1\mathrm{b}_1}(\theta_\mathrm{e}) & L_{\mathrm{c}_1}(\theta_\mathrm{e}) \end{pmatrix} \\
\mathbf{L}_2(\theta_\mathrm{e}) &= \begin{pmatrix} L_{\mathrm{a}_2}(\theta_\mathrm{e}) & M_{\mathrm{a}_2\mathrm{b}_2}(\theta_\mathrm{e}) & M_{\mathrm{a}_2\mathrm{c}_2}(\theta_\mathrm{e}) \\ M_{\mathrm{b}_2\mathrm{a}_2}(\theta_\mathrm{e}) & L_{\mathrm{b}_2}(\theta_\mathrm{e}) & M_{\mathrm{b}_2\mathrm{c}_2}(\theta_\mathrm{e}) \\ M_{\mathrm{c}_2\mathrm{a}_2}(\theta_\mathrm{e}) & M_{\mathrm{c}_2\mathrm{b}_2}(\theta_\mathrm{e}) & L_{\mathrm{c}_2}(\theta_\mathrm{e}) \end{pmatrix} \\
\mathbf{M}_{12}(\theta_\mathrm{e}) &= \begin{pmatrix} M_{\mathrm{a}_1\mathrm{a}_2}(\theta_\mathrm{e}) & M_{\mathrm{a}_1\mathrm{b}_2}(\theta_\mathrm{e}) & M_{\mathrm{a}_1\mathrm{c}_2}(\theta_\mathrm{e}) \\ M_{\mathrm{b}_1\mathrm{a}_2}(\theta_\mathrm{e}) & M_{\mathrm{b}_1\mathrm{b}_2}(\theta_\mathrm{e}) & M_{\mathrm{b}_1\mathrm{c}_2}(\theta_\mathrm{e}) \\ M_{\mathrm{c}_1\mathrm{a}_2}(\theta_\mathrm{e}) & M_{\mathrm{c}_1\mathrm{b}_2}(\theta_\mathrm{e}) & M_{\mathrm{c}_1\mathrm{c}_2}(\theta_\mathrm{e}) \end{pmatrix}
\end{aligned}. \tag{3.16}$$

3.1.1 Leakage inductances

In general, the flux that does not contribute to the electromechanical energy conversion is called leakage flux, and the leakage inductance is the inductance associated with this flux component (Lipo, 2012). According to Krause et al. (2002), the amount of leakage inductance is generally 5 to 10% of the maximum self-inductance. In double-star machines, the leakage inductance limits the harmonic currents that can originate from the voltage supply or from the machine itself (Kanerva et al., 2008). Thus, the computation of stator leakage inductances can be an issue in the design of multiphase machines (Tessarolo and Luise, 2008).

Lipo (2012) divides the leakage inductances into two main categories: the end-winding leakage inductances and the gap leakage inductances. A 2-D FEA is sufficient to take the gap leakage flux into account. Instead, predicting the leakage inductance proportion caused by the stator end-windings is a more challenging task. The end winding is the part of the armature winding that connects the coil sides located in the slots positioned in different pole regions (Ban et al., 2005). The end-winding inductance is generally approximated to be a negligible component of the winding inductance because the end windings are relatively far from the iron parts, but in machines with a low length/diameter ratio, long-pitched windings, or small inherent phase inductances, it may be of a particular importance (Hsieh et al., 2007). The end-winding leakage inductance can be estimated by the following equation (Bianchi, 2002)

$$L_{\sigma\mathrm{s,ew}} = \mu_0 \frac{N^2}{2p} l_\mathrm{ew} \lambda_\mathrm{ew} \tag{3.17}$$

where l_{ew} is the effective end-winding length, and λ_{ew} is a specific permeance coefficient. Hadiouche et al. (2004), instead, have assumed that the end-winding leakage flux distribution around the stator periphery is the same as for the slot leakage flux. In this thesis, the end-winding leakage inductance is omitted, and only the proportion of the leakage flux that is inherently taken into account by the 2-D finite-element analysis is considered in the inductance values.

3.2 Flux produced by PMs

In the modeling of PM machines, another key parameter is the flux produced by the PMs. The PM flux is an important parameter of the PM machine models, since it contributes to the torque production and determines the no-load back electromotive force (EMF).

3.2.1 Fundamental component

At no load, the flux density distribution in the air gap is a function of magnet magnetization and stator tooth and slot structure (Dajaku and Gerling, 2010a). In load conditions, the armature reaction further modifies the flux density distribution. In many cases it is preferred to have a sinusoidal flux density distribution in the air gap. A sinusoidal air-gap flux density can be achieved by placing and forming the magnets appropriately (Jahns and Soong, 1996). In some PM machines, the flux density distribution can also be rectangular.

Figure 3.4 shows six different PM rotor topologies. The magnets can be mounted on the surface of the rotor or buried inside the rotor. Rotor topologies with inset magnets have also been used. In topologies b) and f), the pole shoes are shaped to produce sinusoidal flux density in the air gap. In machines with surface-mounted PMs, the armature reaction is small compared with IPM machines (Heikkilä, 2002).

The surface integral of the air-gap flux density gives the air-gap flux. According to Faraday's induction law, the air-gap flux linkage ψ_{m} induces a voltage in the winding

$$e_{\mathrm{m}} = -\frac{\mathrm{d}\psi_{\mathrm{m}}}{\mathrm{d}t}. \tag{3.18}$$

Assuming that the main flux penetrating a winding varies sinusoidally, the flux linkage can be expressed as

$$\psi_{\mathrm{m}}(t) = \hat{\psi}_{\mathrm{m}} \sin(\omega_{\mathrm{e}} t), \tag{3.19}$$

where ω_{e} is the electrical angular frequency. Taking into account the winding factor k_{w1} of the fundamental component and the number of turns N in the coil, the fundamental wave of the back EMF can be obtained by the following equation

$$e_{\mathrm{m}} = -N k_{\mathrm{w1}} \omega_{\mathrm{e}} \hat{\psi}_{\mathrm{m}} \cos(\omega_{\mathrm{e}} t). \tag{3.20}$$

The flux density distribution and the winding distribution affect the back EMF, and therefore, in some machines the back-EMF waveform can be far from sinusoidal. Even if the flux density distribution and the winding distribution were purely sinusoidal, some amount of harmonics would be present because of the stator slotting (Dajaku and Gerling, 2010b).

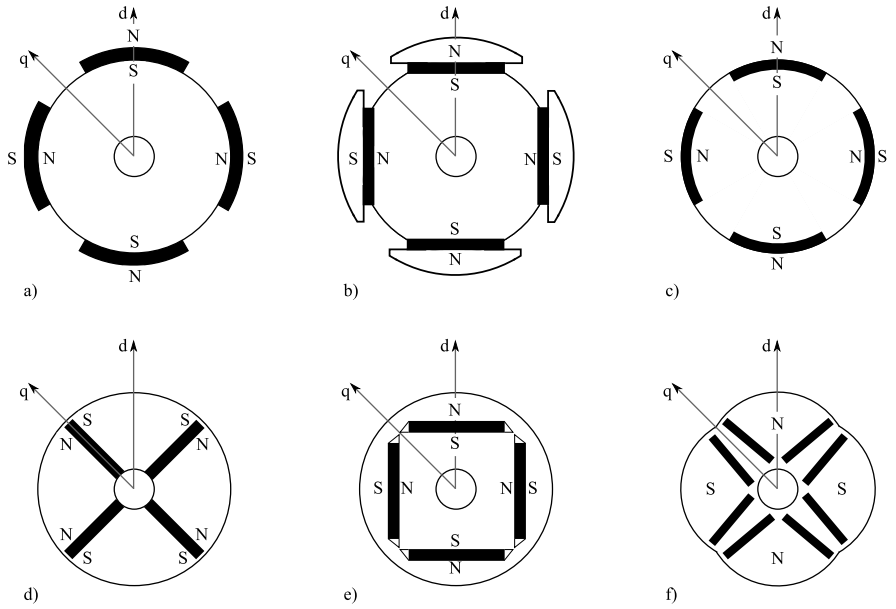

Figure 3.4: Different rotor topologies with permanent magnets producing radial flux; a) and b) surface-mounted PMs; c) inset PMs; d), e), and f) buried PMs. In topologies b) and f) the pole shoes are shaped to produce sinusoidal flux density in the air gap. Adapted from Heikkilä (2002).

3.2.2 Harmonics

Depending on the machine design, the amount of harmonics in the PM flux can be significant, and therefore, they should be considered in order to improve the accuracy of the model. Equation (3.19) can be expanded with the help of a Fourier series expansion to take into account the n harmonics. Thus, the main flux penetrating a winding can be expressed as

$$\psi_{\mathrm{m}} = \sum_{n=1}^{\infty} \hat{\psi}_{\mathrm{m}n} \sin(n\omega_{\mathrm{e}}t + \phi_n). \tag{3.21}$$

The angle ϕ_n defines the displacement angle of the corresponding harmonic component; for the fundamental component $\phi_1 = 0$.

Skewing of the stator (or rotor) improves the distribution of the stator windings, which further decreases the harmonics in the back EMF. Hence, a more sinusoidal back-EMF waveform can be obtained by skewing. Skewing can also be used to decrease the cogging torque. Skewing, however, has also some drawbacks: it decreases the average torque and reduces the fundamental component of the back EMF, and finally, there are some manufacturing problems involved (Jahns and Soong, 1996).

3.3 Conclusion

This chapter introduced the equations of the main parameters of double-star PM machines used in the phase-variable model in Publication I and in the derivation of the decoupled d–q model in Publication II. These parameters include the stator inductances and the flux produced by the PMs. The inductances are the key factors in the machine modeling since they relate the fluxes to the currents. The PM flux is important as it contributes to the torque characteristics of the machine.

Chapter 4

Modeling of double-star PM machines

This chapter discusses the modeling of double-star PM machines by analyzing Publications I and II in brief. The decoupled d–q model derived in Publication II is compared by main elements with existing models, which are obtained by the double d–q winding approach and the vector-space decomposition approach. Further, the decoupled d–q model is represented with space vectors to show the influence of the difference between the d- and q-axes inductances on the voltage equations. Later on, capital DQ letters are used to distinguish the decoupled D–Q reference frames from the three-phase d–q reference frame.

4.1 Publication I – Phase-variable model

The key issues on the modeling of double-star PM machines are rotor position dependent inductances, mutual couplings, and harmonics. Publication I studies the effect of inductance harmonics and PM flux harmonics using a finite-element-based phase-variable model. For the simulation and analysis of conventional three-phase machine drives, a phase-variable model has been proposed in Mohammed et al. (2004). Later in Mohammed et al. (2007), the model was extended to take into account also fault conditions. The phase-variable model provides the same performance in particular operating point as the full application of FE models but with a much faster simulation speed (Mohammed et al., 2004). It is expected that the phase-variable model for double-star PM machines provides the same advantages. In Publication I the emphasis is on the model correspondence with the finite-element analysis taking into account the inductance and PM flux harmonics, and thus, the simulation speeds are not compared.

The phase-variable model is based directly on the voltage equations of electrical machines

$$\mathbf{U} = \mathbf{R}\mathbf{I} + \frac{\mathrm{d}\boldsymbol{\Psi}}{\mathrm{d}t}, \tag{4.1}$$

where, in the case of PM machines, the flux linkage is defined as

$$\boldsymbol{\Psi} = \mathbf{L}\mathbf{I} + \boldsymbol{\Psi}_{\mathrm{PM}}. \tag{4.2}$$

Substituting (4.2) into (4.1) yields

$$\mathbf{E} = (\mathbf{R} + p\mathbf{L} + \mathbf{L}p) \cdot \mathbf{I} - \mathbf{U} \tag{4.3}$$

where p is the time derivative operator and $\mathbf{E}$ is the no-load EMF. The model is constructed without any transformations, and thus, the inductance harmonics as well as the harmonics in the flux produced by the PMs can be easily included in the model. The clear drawback of the model is that the PM flux and the inductances have to be determined as a function of rotor position, and thus, the model becomes more complex. Although the data can be obtained straightforwardly by using a finite-element analysis, its construction by using look-up tables can be time consuming. Analytical approaches to calculate the winding inductances can also be adopted (Obe, 2009), but for saturated conditions the FEM is preferred.

4.1.1 Effect of Harmonics

In Publication I, an example double-star machine, in which the two three-phase winding sets are displaced by 30 electrical degrees, is supplied with sinusoidal voltages in order to generate only machine-based harmonics. The inductance and no-load PM flux parameters are obtained from finite-element analyses by using ANSYS Maxwell. Four cases are considered as included in the model:

1. only fundamental components (case 1),
2. back-EMF harmonics (case 2),
3. inductance harmonics (case 3), and
4. both above-mentioned harmonics (case 4).

Cases 1 and 2 produce nearly sinusoidal curves with a negligible harmonic content. Instead, in cases 3 and 4, where the inductance harmonics ($n = 1, 2, \ldots$,7) are taken into account, the currents contain a notable amount of harmonics. Moreover, compared with cases 1 and 2, the current curves in cases 3 and 4 have better correspondence with the FEA current curve. Clearly, the accuracy of the model is improved by taking into account the inductance harmonics. In this example machine, the inductance harmonics have a significant effect, whereas the back-EMF harmonics have only a minor effect on the current curves.

4.2 Publication II – Decoupled D–Q reference frames

The number of electrical differential equations required to describe the behavior of an electrical machine depends on the number of independent electrical variables, which are either currents or fluxes. The number of independent variables is not affected by the mathematical transformation; in other words, although the phase-variable model of a multiphase machine is transformed, the number of independent variables must remain the same (Levi, 2008).

The transformation matrix derived in Publication II for double-star salient-pole machines with an arbitrary displacement angle between the winding sets is as follows (Kallio et al., 2013)

$$\mathbf{T}_{\mathrm{DQ}}(\theta) = \frac{1}{\sqrt{2}} \begin{pmatrix} \mathbf{T}_{\mathrm{P}}(\theta + \alpha) & \mathbf{T}_{\mathrm{P}}(\theta - \alpha) \\ \mathbf{T}_{\mathrm{P}}(\theta + \alpha + \frac{\pi}{2}) & \mathbf{T}_{\mathrm{P}}(\theta - \alpha - \frac{\pi}{2}) \end{pmatrix} \tag{4.4}$$

where $\mathbf{T}_{\mathrm{P}}(\delta)$ is the Park transformation with power-invariant scaling. Note that the zero sequence components have been omitted, and thus, (4.4) is a 4×6 matrix. Applying (4.4) to the phase-variable model of double-star electrical machines (4.3) results in

$$\mathbf{E}_{\mathrm{DQ}} = (\mathbf{R}_{\mathrm{DQ}} + p\mathbf{L}_{\mathrm{DQ}} + \omega\mathbf{J} \cdot \mathbf{L}_{\mathrm{DQ}} + \mathbf{L}_{\mathrm{DQ}}p) \cdot \mathbf{I}_{\mathrm{DQ}} - \mathbf{U}_{\mathrm{DQ}} \tag{4.5}$$

where the $\mathbf{J}$ matrix is as follows

$$\begin{aligned} \mathbf{J} &= \mathbf{T}_{\mathrm{DQ}}(\theta) \cdot \frac{\mathrm{d}}{\mathrm{d}\theta} \mathbf{T}_{\mathrm{DQ}}(\theta)^{\mathrm{T}} \\ &= \begin{pmatrix} 0 & -1 & 0 & 0 \\ 1 & 0 & 0 & 0 \\ 0 & 0 & 0 & -1 \\ 0 & 0 & 1 & 0 \end{pmatrix}. \end{aligned} \tag{4.6}$$

The $\mathbf{J}$ matrix is a constant matrix and causes no coupling between the two reference frames. Note that the term $p\mathbf{L}_{\mathrm{DQ}}$ in (4.5) can be eliminated because the elements of $\mathbf{L}_{\mathrm{DQ}}$ are constants.

Figure 4.1 illustrates the decoupled D–Q reference frames. In the representation of the D_2–Q_2 reference frame (see Figure 4.1(b)), the rotor is depicted by a dashed line, because fixing the reference frame to the rotor is unnecessary. Moreover, if $\alpha = 0^\circ$ or $\alpha = 30^\circ$ and even harmonics are neglected, the phase variables do not map into the D_2–Q_2 reference frame. Instead, if $\alpha = 15^\circ$, certain harmonics map into the D_2–Q_2 frame but they rotate only in the stator and do not contribute to the torque. Mapping of the harmonics is further discussed in Section 4.2.4.

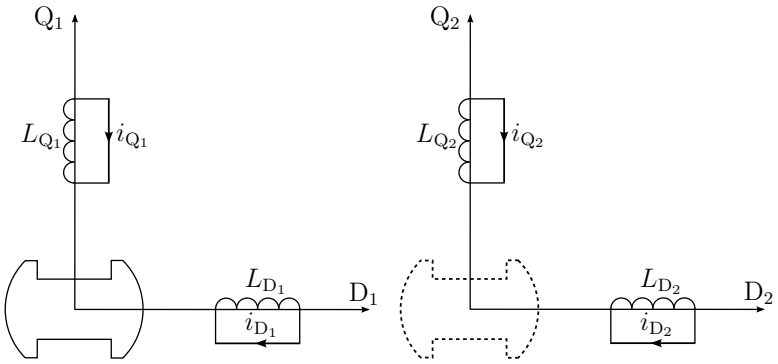

(a) D_1–Q_1 reference frame (b) D_2–Q_2 reference frame

Figure 4.1: Decoupled D–Q reference frames; no coupling between the reference frames occurs. In (b) the rotor is depicted by a dashed line as it can be omitted. (Publication III)

4.2.1 Stator model

The stator model (the stator flux linkages) is obtained by applying (4.4) to (4.2)

$$\begin{aligned}
\psi_{\mathrm{D}_1} &= L_{\mathrm{D}_1} i_{\mathrm{D}_1} + \psi_{\mathrm{PM,D}_1} \\
\psi_{\mathrm{Q}_1} &= L_{\mathrm{Q}_1} i_{\mathrm{Q}_1} \\
\psi_{\mathrm{D}_2} &= L_{\mathrm{D}_2} i_{\mathrm{D}_2} \\
\psi_{\mathrm{Q}_2} &= L_{\mathrm{Q}_2} i_{\mathrm{Q}_2}.
\end{aligned} \tag{4.7}$$

The fundamental component of the PM flux is aligned on the D_1-axis. Application of (4.4) to the phase-variable inductance waveforms presented in Chapter 3 maps the constant and second-harmonic inductance coefficients into the D–Q reference frames as follows

$$\begin{aligned}
L_{\mathrm{D1}} &= L_{\mathrm{s0}} + \frac{L_{\mathrm{s2}}}{2} - M_{\mathrm{s0}} + M_{\mathrm{s2}} + \frac{1}{2}(3M_{\mathrm{m0}} + M_{\mathrm{m2}}) \\
L_{\mathrm{Q1}} &= L_{\mathrm{s0}} - \frac{L_{\mathrm{s2}}}{2} - M_{\mathrm{s0}} - M_{\mathrm{s2}} + \frac{1}{2}(3M_{\mathrm{m0}} - M_{\mathrm{m2}}) \\
L_{\mathrm{D2}} &= L_{\mathrm{s0}} - \frac{L_{\mathrm{s2}}}{2} - M_{\mathrm{s0}} - M_{\mathrm{s2}} - \frac{1}{2}(3M_{\mathrm{m0}} - M_{\mathrm{m2}}) \\
L_{\mathrm{Q2}} &= L_{\mathrm{s0}} + \frac{L_{\mathrm{s2}}}{2} - M_{\mathrm{s0}} + M_{\mathrm{s2}} - \frac{1}{2}(3M_{\mathrm{m0}} + M_{\mathrm{m2}}).
\end{aligned} \tag{4.8}$$

The inductances represented in the decoupled D–Q reference frames are constant and do not depend on the rotor position. It is evident that if the second harmonic coefficients are zero, the inductances result in $L_{\mathrm{D}_1} = L_{\mathrm{Q}_1}$ and $L_{\mathrm{D}_2} = L_{\mathrm{Q}_2}$, which denotes non-salient pole machines. In interior permanent magnet machines all the second harmonic coefficients are negative, which results in $L_{\mathrm{Q1}} > L_{\mathrm{D1}}$. The D_2–Q_2 frame inductances are different in that regard as they can result in same values also in the case of IPM machines (if $L_{\mathrm{s2}} = M_{\mathrm{m2}} - 2M_{\mathrm{s2}}$, then $L_{\mathrm{D}_2} = L_{\mathrm{Q}_2}$).

4.2.2 Rotor model

The rotor model considering the fundamental components only can be defined simply with the no-load flux linkage $\psi_{\mathrm{PM,D}_1}$ produced by the permanent magnets. The PMs, however, can be represented with an equivalent rotor winding supplied by a constant current I_{f}, and the harmonics in the no-load flux can be included in the rotor model by considering that the no-load flux harmonics are formed by the mutual inductances $M_{\mathrm{fs}}(\delta)$ supplied by the current I_{f} (Andriollo et al., 2009):

$$M_{\mathrm{fs}}(\delta) = \frac{\psi_{\mathrm{fs}}(\delta)}{I_{\mathrm{f}}}. \tag{4.9}$$

The mutual inductances can be expressed in the form

$$M_{\mathrm{fs}}(\delta) = \sum_{n=1}^{\infty} M_{\mathrm{f}n} \cos(n\delta + \phi_n), \tag{4.10}$$

and for the transformation it is necessary to define them in a vector form

$$\mathbf{M}_{\mathrm{fs}}(\theta) = \begin{pmatrix} M_{\mathrm{fs}}(\theta+\alpha) \\ M_{\mathrm{fs}}(\theta+\alpha-2\pi/3) \\ M_{\mathrm{fs}}(\theta+\alpha+2\pi/3) \\ M_{\mathrm{fs}}(\theta-\alpha) \\ M_{\mathrm{fs}}(\theta-\alpha-2\pi/3) \\ M_{\mathrm{fs}}(\theta-\alpha+2\pi/3) \end{pmatrix}. \tag{4.11}$$

Application of (4.4) to (4.11) results in

$$\begin{aligned} M_{\mathrm{fD_1}}(\theta) &= \sqrt{3} \sum_{k=0,\pm1,\pm2}^{\infty} M_{\mathrm{f}|1+3k|} \cos(3k\alpha) \cos(3k\theta + \phi_{|1+3k|}) \\ M_{\mathrm{fQ_1}}(\theta) &= \sqrt{3} \sum_{k=0,\pm1,\pm2}^{\infty} M_{\mathrm{f}|1+3k|} \cos(3k\alpha) \sin(3k\theta + \phi_{|1+3k|}) \\ M_{\mathrm{fD_2}}(\theta) &= \sqrt{3} \sum_{k=0,\pm1,\pm2}^{\infty} M_{\mathrm{f}|1+3k|} \sin(3k\alpha) \cos(3k\theta + \phi_{|1+3k|}) \\ M_{\mathrm{fQ_2}}(\theta) &= \sqrt{3} \sum_{k=0,\pm1,\pm2}^{\infty} M_{\mathrm{f}|1+3k|} \sin(3k\alpha) \sin(3k\theta + \phi_{|1+3k|}) \end{aligned} \tag{4.12}$$

Multiplying (4.12) with the constant current I_{f}, the no-load flux linkages in the $\mathrm{D_1}$–$\mathrm{Q_1}$ and $\mathrm{D_2}$–$\mathrm{Q_2}$ reference frames are obtained. With this procedure, the rotor-based harmonics can be taken into account in the decoupled D–Q model of double-star PM machines.

4.2.3 Complex representation

To operate with space vectors instead of real values, the proposed double-star machine model can be represented by complex space vectors. In general, the model of an electric machine is a multiple-input/multiple-output system that can be simplified to an equivalent single-input/single-output complex vector system by using a complex vector notation (Briz et al., 2000). Although the complex vector representation is appropriate only to electric machines whose rotors are magnetically isotropic (Huh, 2008), it is used here to show the influence of the difference between the D- and Q-axes inductances on the voltage equations.

The electrical variables can be represented in a complex form as follows:

$$\begin{aligned} \vec{f_1} &= f_{\mathrm{D_1}} + \mathrm{j} f_{\mathrm{Q_1}} \\ \vec{f_2} &= f_{\mathrm{D_2}} + \mathrm{j} f_{\mathrm{Q_2}} \end{aligned} \tag{4.13}$$

where f denotes either *u*, *i*, ψ, *e*, or *L*. In order to represent the transformation matrices in a complex form, the complex 1×3 vector needs to be introduced

$$\bar{\mathbf{c}} = e^{-\mathrm{j}\theta} \begin{pmatrix} 1 & e^{\mathrm{j}2\pi/3} & e^{\mathrm{j}4\pi/3} \end{pmatrix}. \tag{4.14}$$

The Park transformation matrix that transforms electrical variables of two three-phase windings

(displaced by 2α) into a double d–q reference frame is expressed as

$$\overline{\mathbf{T}}_{\mathrm{dq}}(\theta) = \sqrt{\frac{2}{3}} \begin{pmatrix} e^{-\mathrm{j}\alpha}\overline{\mathbf{c}} & \mathbf{0}_{1,3} \\ \mathbf{0}_{1,3} & e^{\mathrm{j}\alpha}\overline{\mathbf{c}} \end{pmatrix} \tag{4.15}$$

with $\mathbf{0}_{1,3}$ is a 1×3 vector with all the elements zero. The transformation matrix that diagonalizes the stator inductance matrix after application of (4.15) to (3.15) can be expressed in a complex form as follows

$$\overline{\mathbf{T}}_{\mathrm{diag}} = \frac{1}{\sqrt{2}} \begin{pmatrix} e^{\mathrm{j}0} & e^{\mathrm{j}0} \\ e^{-\mathrm{j}\frac{\pi}{2}} & e^{\mathrm{j}\frac{\pi}{2}} \end{pmatrix}. \tag{4.16}$$

The final transformation matrix is obtained by combining (4.15) and (4.16), and thus

$$\overline{\mathbf{T}}_{\mathrm{DQ}}(\theta) = \frac{1}{\sqrt{3}} \left(\begin{array}{c|c} e^{-\mathrm{j}\alpha}\overline{\mathbf{c}} & e^{\mathrm{j}\alpha}\overline{\mathbf{c}} \\ \hline e^{-\mathrm{j}(\alpha+\pi/2)}\overline{\mathbf{c}} & e^{\mathrm{j}(\alpha+\pi/2)}\overline{\mathbf{c}} \end{array} \right). \tag{4.17}$$

Converting (4.5) into two scalar complex equations results in

$$\begin{aligned} \vec{e}_1 &= (R_{\mathrm{s}} + \mathrm{j}\omega L_{\mathrm{D}_1} + L_{\mathrm{D}_1}p)\,\vec{i}_1 + \Delta L_1(\omega - \mathrm{j}p)i_{\mathrm{Q}_1} - \vec{u}_1 \\ \vec{e}_2 &= (R_{\mathrm{s}} + \mathrm{j}\omega L_{\mathrm{D}_2} + L_{\mathrm{D}_2}p)\,\vec{i}_2 + \Delta L_2(\omega - \mathrm{j}p)i_{\mathrm{Q}_2} - \vec{u}_2, \end{aligned} \tag{4.18}$$

where the back-EMF waveforms including the harmonics in the PM flux are expressed as

$$\begin{aligned} \vec{e}_1 &= -(p + \mathrm{j}\omega)\vec{\psi}_1(\theta) \\ \vec{e}_2 &= -(p + \mathrm{j}\omega)\vec{\psi}_2(\theta) \end{aligned} \tag{4.19}$$

with

$$\begin{aligned} \vec{\psi}_1(\theta) &= \sqrt{3}I_{\mathrm{f}} \sum_{k=0,\pm1,\pm2}^{\infty} M_{\mathrm{f}|1+3k|} \cos(3k\alpha) e^{j(3k\theta+\phi_{|1+3k|})} \\ \vec{\psi}_2(\theta) &= \sqrt{3}I_{\mathrm{f}} \sum_{k=0,\pm1,\pm2}^{\infty} M_{\mathrm{f}|1+3k|} \sin(3k\alpha) e^{j(3k\theta+\phi_{|1+3k|})}, \end{aligned} \tag{4.20}$$

and

$$\begin{aligned} \Delta L_1 &= L_{\mathrm{D}_1} - L_{\mathrm{Q}_1} \\ \Delta L_2 &= L_{\mathrm{D}_2} - L_{\mathrm{Q}_2}. \end{aligned} \tag{4.21}$$

Equation (4.18) results in exactly the same form as originally presented by Andriollo et al. (2009) for non-salient pole PM machines, if $L_{\mathrm{D}_1} = L_{\mathrm{Q}_1}$ and $L_{\mathrm{D}_2} = L_{\mathrm{Q}_2}$, as is the case for non-salient pole machines. The complex form representation of double-star IPM machines modeled in the decoupled D–Q reference frames includes additional terms which show the influence of the reluctance differences between the D- and Q-axes. Obviously, the effect of the reluctance differences depends on the rotational speed ω. In addition, the reluctance differences are associated with the Q-axes currents only. Because of the reluctance difference, the voltage equations expressed with complex vectors cannot be simplified further, and thus a more compact representation is obtained by the matrix representation (4.5).

4.2.4 Mapping of harmonics

Publication II discusses the mapping of harmonics when the displacement between the winding sets is 30 electrical degrees: the fundamental wave and the $(12k\pm1)$th harmonics $(k = 1, 2, 3, \ldots)$ in the original quantities are mapped into the D_1–Q_1 reference frame, and the $(6(2k + 1) \pm 1)$th harmonics $(k = 0, 1, 2, \ldots)$ are mapped into the D_2–Q_2 reference frames. For the general displacement angle we may consider a vector of the form

$$\mathbf{f}_n = \begin{pmatrix} A_n \sin(n(\theta+\alpha)+\phi_n) \\ A_n \sin(n(\theta+\alpha-2\pi/3)+\phi_n) \\ A_n \sin(n(\theta+\alpha+2\pi/3)+\phi_n) \\ A_n \sin(n(\theta-\alpha)+\phi_n) \\ A_n \sin(n(\theta-\alpha-2\pi/3)+\phi_n) \\ A_n \sin(n(\theta-\alpha+2\pi/3)+\phi_n) \end{pmatrix} \tag{4.22}$$

where n is the order of harmonic ($n = 1, -5, 7, -11, 13, ...$), A_n is the peak value of the corresponding harmonic component, and ϕ_n is the harmonic displacement angle.

Considering first the fundamental component ($n = 1$), the application of (4.4) to (4.22) results in

$$n = 1 \begin{cases} f_{\mathrm{D}_1} = \sqrt{3}A_1 \sin(\phi_1) \\ f_{\mathrm{Q}_1} = -\sqrt{3}A_1 \cos(\phi_1) \\ f_{\mathrm{D}_2} = 0 \\ f_{\mathrm{Q}_2} = 0 \end{cases} \tag{4.23}$$

Hence, the fundamental component is always mapped into the D_1–Q_1 reference frame independently of the displacement angle 2α between the winding sets. The 5th and 7th harmonics, instead, map into the D–Q reference frames as follows

$$n = -5 \begin{cases} f_{\mathrm{D}_1} = -\sqrt{3}A_5 \cos(6\alpha)\sin(6\theta-\phi_5) \\ f_{\mathrm{Q}_1} = -\sqrt{3}A_5 \cos(6\alpha)\cos(6\theta-\phi_5) \\ f_{\mathrm{D}_2} = \sqrt{3}A_5 \sin(6\alpha)\sin(6\theta-\phi_5) \\ f_{\mathrm{Q}_2} = \sqrt{3}A_5 \sin(6\alpha)\cos(6\theta-\phi_5) \end{cases} \tag{4.24}$$

and

$$n = 7 \begin{cases} f_{\mathrm{D}_1} = \sqrt{3}A_7 \cos(6\alpha)\sin(6\theta+\phi_7) \\ f_{\mathrm{Q}_1} = -\sqrt{3}A_7 \cos(6\alpha)\cos(6\theta+\phi_7) \\ f_{\mathrm{D}_2} = \sqrt{3}A_7 \sin(6\alpha)\sin(6\theta+\phi_7) \\ f_{\mathrm{Q}_2} = -\sqrt{3}A_7 \sin(6\alpha)\cos(6\theta+\phi_7) \end{cases} \tag{4.25}$$

whereas the 11th and 13th harmonics map as follows:

$$n = -11 \begin{cases} f_{\mathrm{D}_1} = -\sqrt{3}A_{11} \cos(12\alpha)\sin(12\theta-\phi_{11}) \\ f_{\mathrm{Q}_1} = -\sqrt{3}A_{11} \cos(12\alpha)\cos(12\theta-\phi_{11}) \\ f_{\mathrm{D}_2} = \sqrt{3}A_{11} \sin(12\alpha)\sin(12\theta-\phi_{11}) \\ f_{\mathrm{Q}_2} = \sqrt{3}A_{11} \sin(12\alpha)\cos(12\theta-\phi_{11}) \end{cases} \tag{4.26}$$

and

$$n = 13 \begin{cases} f_{\mathrm{D}_1} = \sqrt{3} A_{13} \cos(12\alpha) \sin(12\theta + \phi_{13}) \\ f_{\mathrm{Q}_1} = -\sqrt{3} A_{13} \cos(12\alpha) \cos(12\theta + \phi_{13}) \\ f_{\mathrm{D}_2} = \sqrt{3} A_{13} \sin(12\alpha) \sin(12\theta + \phi_{13}) \\ f_{\mathrm{Q}_2} = -\sqrt{3} A_{13} \sin(12\alpha) \cos(12\theta + \phi_{13}) \end{cases} \tag{4.27}$$

Table 4.1 illustrates the mapping of the fundamental component and harmonics of the order 5, 7, 11, and 13 into the D–Q reference frames with different values of α. Note that α is defined as the half of the displacement angle between the winding sets.

Table 4.1: Mapping of the fundamental component and harmonics of the order 5, 7, 11, and 13 into the D–Q reference frames in symmetrical load conditions. The numbers in bold refer to that the magnitude of the corresponding harmonic is greater in the reference frame at issue.

α	D_1–Q_1 reference frame	D_2–Q_2 reference frame
$0°$	1, 5, 7, 11, 13	–
$3.75°$	1, **5**, **7**, 11, 13	5, 7, 11, 13
$7.5°$	1, 5, 7	5, 7, 11, 13
$11.25°$	1, 5, 7, 11, 13	**5**, **7**, 11, 13
$15°$	1, 11, 13	5, 7
$18.75°$	1, 5, 7, 11, 13	**5**, **7**, 11, 13
$22.5°$	1, 5, 7	5, 7, 11, 13
$26.25°$	1, **5**, **7**, 11, 13	5, 7, 11, 13
$30°$	1, 5, 7, 11, 13	–

The fundamental component maps always into the D_1–Q_1 reference frame as (4.23) shows. If the winding sets are equal in phase (i.e., $\alpha = 0°$) or displaced by $\alpha = 30°$ (symmetrical six-phase machine), all the harmonics map into the D_1–Q_1 frame and none into the D_2–Q_2 frame. By selecting $\alpha = 7.5°$ or $\alpha = 22.5°$ the 11th and 13th harmonics map only into the D_2–Q_2 reference frame. If $\alpha = 15°$, the 5th and 7th harmonics do not contribute to the D_1–Q_1 frame variables. On the contrary, in that case the 11th and 13th harmonics are mapped only into the D_1–Q_1 frame. Thus, selecting the displacement angle $\alpha = 15°$ results in the highest harmonic frequency components in the D_1–Q_1 frame.

4.3 Comparison with existing methods

4.3.1 Double d–q winding approach

The double d–q reference frames are obtained with the following transformation matrix

$$\mathbf{T}_{\mathrm{dq}}(\theta) = \begin{pmatrix} \mathbf{T}_{\mathrm{P}}(\theta + \alpha) & \mathbf{0}_{2,3} \\ \mathbf{0}_{2,3} & \mathbf{T}_{\mathrm{P}}(\theta - \alpha) \end{pmatrix} \tag{4.28}$$

where $\mathbf{T}_{\mathrm{P}}(\delta)$ is the Park transformation matrix (2.1) without the last row, which takes into account the zero-sequence component. Assuming that the windings are equal and considering only fundamental (constant and second-harmonic) components of phase-variable inductances, the application of (4.28) to the stator inductance matrix $\mathbf{L}(\theta)$ (3.15) results in

$$\begin{aligned}\mathbf{L}_{\mathrm{dq}} &= \mathbf{T}_{\mathrm{dq}}(\theta) \cdot \mathbf{L}(\theta) \cdot \mathbf{T}_{\mathrm{dq}}^{\mathrm{T}}(\theta) \\ &= \begin{pmatrix} L_{\mathrm{d}} & 0 & M_{\mathrm{d}} & 0 \\ 0 & L_{\mathrm{q}} & 0 & M_{\mathrm{q}} \\ M_{\mathrm{d}} & 0 & L_{\mathrm{d}} & 0 \\ 0 & M_{\mathrm{q}} & 0 & L_{\mathrm{q}} \end{pmatrix},\end{aligned} \tag{4.29}$$

where L_{d} and L_{q} are the d–q reference frame inductances of the winding sets, and M_{d} and M_{q} are the d–q reference frame mutual inductances that are due to the coupling between the d–q frames. The elements of (4.29) do not depend on the rotor position, and thus, the rotor position dependency of inductances is eliminated with the double d–q winding approach. However, there are mutual couplings between the d–q frames. Figure 4.2 illustrates the mutual couplings.

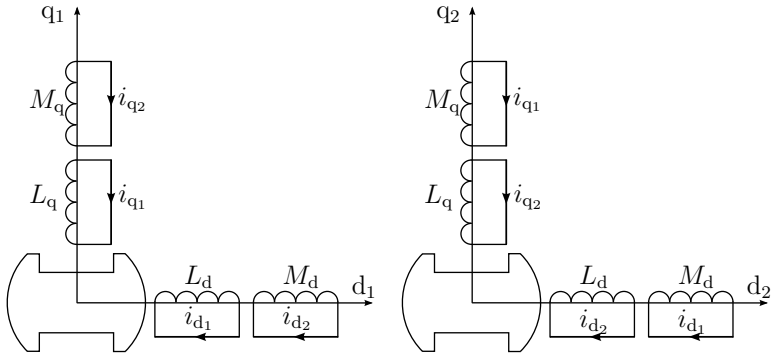

(a) $\mathrm{d_1}$–$\mathrm{q_1}$ reference frame (b) $\mathrm{d_2}$–$\mathrm{q_2}$ reference frame

Figure 4.2: Double d–q reference frames. The mutual couplings between the frames are illustrated by the mutual inductances M_{d} and M_{q}.

The stator flux linkages in the $\mathrm{d_1}$–$\mathrm{q_1}$ and $\mathrm{d_2}$–$\mathrm{q_2}$ reference frames (obtained by multiplying (4.2) by (4.28)) illustrate the mutual couplings further

$$\begin{aligned}\psi_{\mathrm{d_1}} &= L_{\mathrm{d}} i_{\mathrm{d_1}} + M_{\mathrm{d}} i_{\mathrm{d_2}} + \psi_{\mathrm{PM}} \\ \psi_{\mathrm{q_1}} &= L_{\mathrm{q}} i_{\mathrm{q_1}} + M_{\mathrm{q}} i_{\mathrm{q_2}} \\ \psi_{\mathrm{d_2}} &= L_{\mathrm{d}} i_{\mathrm{d_2}} + M_{\mathrm{d}} i_{\mathrm{d_1}} + \psi_{\mathrm{PM}} \\ \psi_{\mathrm{q_2}} &= L_{\mathrm{q}} i_{\mathrm{q_2}} + M_{\mathrm{q}} i_{\mathrm{q_1}}.\end{aligned} \tag{4.30}$$

The above equations suggest that in order to calculate the flux linkage for example in the $\mathrm{d_1}$-axis, the inductance L_{d}, the current $i_{\mathrm{d_1}}$ and flux linkage ψ_{PM}, and the mutual inductance M_{d} linking the two d-axes and the current in the second d-axis are needed. Equation (4.30) also suggests that if only one winding set is loaded, the flux linkages in the other d–q reference frame will not be zero even if the flux produced by the PMs is omitted. Consequently, because of the mutual coupling,

the double d–q reference frame is not the optimal reference frame for control design purposes of double-star PM machines.

4.3.2 Vector space decomposition approach

The vector space decomposition (VSD) approach proposed by Zhao and Lipo (1995) is commonly used in modeling and control of double-star machines in which the displacement between the two winding sets is 30 electrical degrees ($\alpha = 15^\circ$). Application of the VSD transformation (2.4) (without the last two rows) to the stator inductance matrix $\mathbf{L}(\theta)$ (3.15) when $\alpha = 15^\circ$ results in

$$\begin{aligned}\mathbf{L}_{\mathrm{VSD}} &= \mathbf{T} \cdot \mathbf{L}(\theta) \cdot \mathbf{T}^{\mathrm{T}} \\ &= \begin{pmatrix} L_\alpha(\theta) & M_{\alpha\beta}(\theta) & 0 & 0 \\ M_{\alpha\beta}(\theta) & L_\beta(\theta) & 0 & 0 \\ 0 & 0 & L_{\mathrm{x}}(\theta) & M_{\mathrm{xy}}(\theta) \\ 0 & 0 & M_{\mathrm{xy}}(\theta) & L_{\mathrm{y}}(\theta) \end{pmatrix},\end{aligned} \tag{4.31}$$

where

$$\begin{aligned} L_\alpha &= L_{\mathrm{s0}} - M_{\mathrm{s0}} + \frac{3}{2}M_{\mathrm{m0}} + \frac{1}{2}\cos(2\theta)(L_{\mathrm{s2}} + 2M_{\mathrm{s2}} + M_{\mathrm{m2}}), \\ L_\beta &= L_{\mathrm{s0}} - M_{\mathrm{s0}} + \frac{3}{2}M_{\mathrm{m0}} - \frac{1}{2}\cos(2\theta)(L_{\mathrm{s2}} + 2M_{\mathrm{s2}} + M_{\mathrm{m2}}), \\ M_{\alpha\beta} &= \cos(\theta)\sin(\theta)(L_{\mathrm{s2}} + 2M_{\mathrm{s2}} + M_{\mathrm{m2}}), \\ L_{\mathrm{x}} &= L_{\mathrm{s0}} - M_{\mathrm{s0}} - \frac{3}{2}M_{\mathrm{m0}} + \frac{1}{2}\cos(2\theta)(L_{\mathrm{s2}} + 2M_{\mathrm{s2}} - M_{\mathrm{m2}}), \\ L_{\mathrm{y}} &= L_{\mathrm{s0}} - M_{\mathrm{s0}} - \frac{3}{2}M_{\mathrm{m0}} + \frac{1}{2}\cos(2\theta)(M_{\mathrm{m2}} - L_{\mathrm{s2}} - 2M_{\mathrm{s2}}), \\ M_{\mathrm{xy}} &= \cos(\theta)\sin(\theta)(M_{\mathrm{m2}} - L_{\mathrm{s2}} - 2M_{\mathrm{s2}}). \end{aligned} \tag{4.32}$$

The elements of (4.31) depend on the rotor position because the VSD transformation maps variables into stationary reference frames α–β and x–y. The two reference frames, on the other hand, are clearly uncoupled. The α–β reference frame is commonly rotationally transformed to d–q (synchronously rotating) reference frame in which the fundamental components becomes DC quantities and which is more suitable for vector control (Levi et al., 2007). Instead, the x–y reference frame is not transformed to synchronously rotating reference frame because the x–y reference frame variables do not contribute to the electromechanical energy conversion (Che et al., 2014). If the second-harmonic inductance coefficients are zero, the matrix (4.31) results in a diagonal matrix where the diagonal elements do not depend on the rotor position and where $L_\alpha = L_\beta$ and $L_{\mathrm{x}} = L_{\mathrm{y}}$. Thus, application of the rotational transformation is of no importance. In the case of double-star IPM machines the stator inductances depend on the rotor position and therefore the both reference frames need to be rotationally transformed.

The dependency of the parameters on the rotor position can be eliminated by transforming the

matrix (4.31) by using a rotation transformation

$$\mathbf{T}_{\mathrm{rot}} = \begin{pmatrix} \cos(\theta) & \sin(\theta) & 0 & 0 \\ -\sin(\theta) & \cos(\theta) & 0 & 0 \\ 0 & 0 & \cos(\theta) & -\sin(\theta) \\ 0 & 0 & \sin(\theta) & \cos(\theta) \end{pmatrix}. \tag{4.33}$$

Note that the two reference frames have to be rotated in different directions: The transformation of the α–β reference frame variables to the d–q frame variables is identical to the transformation of a three-phase system (Lipo, 2012). The x–y reference frame instead need to be rotated into counter synchronous direction. The rotation of the x–y reference frame in the counter synchronous direction has also been proposed in (Che et al., 2012) for induction machines at asymmetrical load conditions. The rotation transformation (4.33) diagonalizes the matrix (4.31) and eliminates the rotor position dependency. The resulting diagonal elements correspond with the inductances in (4.8) with the exception that the D_2–Q_2 reference frame inductances are the other way round. The transformation proposed in this thesis is derived based on the diagonalization of the stator inductance matrix of double-star IPM machines and thus it directly results in two decoupled reference frames with inductances that do not depend on the rotor position.

4.4 Conclusion

This chapter discussed modeling of double-star PM machines using a phase-variable model and a decoupled D–Q model that was derived through inductance matrix diagonalization. Models for the rotor and stator sections were introduced. The proposed decoupled D–Q model was also represented by complex vectors. Such a representation has its advantages, such as compactness and generality, when considering non-salient pole machines. Here, the complex vector representation is used to show the influence of the difference between the D- and Q-axes inductances on the voltage equations.

Mapping of harmonics in phase-variable waveforms into the decoupled D–Q reference frames were also discussed. The harmonics map differently into the decoupled D–Q reference frames depending on the harmonic order and the displacement angle α. All the considered harmonics map into the first D–Q reference frame only, when the displacement between the sets is 0° or 60°. The 5th and 7th harmonics map entirely to the second D–Q reference frame by selecting the displacement between the sets as 30°.

The double d–q winding approach and the vector space decomposition (VSD) approach were also described in brief for comparison with the proposed decoupled D–Q transformation. The double d–q winding approach eliminates the rotor-position dependence of inductances but does not eliminate the mutual coupling. The mutual couplings in the double d–q frames complicate the machine control and may have a significant effect on the dynamic performance of the electric drive. The VSD approach that maps the variables into stationary reference frames, instead, does not eliminate the rotor-position dependence of inductances. However, the reference frame that contributes to the electromechanical energy conversion is commonly further transformed with a rotational transformation. In the case of double-star IPM machines the both reference frames have to be rotationally transformed in order to eliminate the rotor position dependence of inductances. However, rotational transformation of the second reference frame to the synchronous direction does not result

in constant inductances. Instead, the reference frame has to be rotated in counter synchronous direction.

The proposed decoupled D–Q reference frames that were derived through inductance matrix diagonalization consider the inductance parameters as constants, and consequently no further rotational transformations are required.

Chapter 5

Determination of machine parameters

The knowledge of the model parameters is of importance in the design and implementation of high-performance vector-controlled drives. Moreover, the machine parameters are needed for analysis and simulation purposes. The proposed analytical model of double-star PM machines consists of the following parameters: the flux produced by PMs ψ_{PM}, the stator resistance R_{s}, and four inductances L_{D_1}, L_{Q_1}, L_{D_2}, and L_{Q_2}. Thus, six parameters are to be determined. The machine parameters can be determined at the design stage, but sometimes the parameters need to be determined afterwards because the parameters of the machine may vary with the operating point (Boileau et al., 2011) or as a result of ageing processes (Valverde et al., 2011) or the parameters are unknown.

This chapter outlines Publications III and IV that address the determination of double-star PM machine parameters by using finite-element analyses (FEAs) and measurements with voltage-source inverters (VSIs). In addition, an AC standstill test is evaluated for this particular machine type. In Publication III, three simple yet accurate methods for determining inductance values in the decoupled D–Q reference frames are proposed. The methods are referred to as off-line methods. Publication IV, instead, proposes an on-line estimation method to update the inductances and the PM flux in different load conditions. The stator resistance and initial values of the inductances are estimated at a standstill, which is considered a special condition in the on-line estimation scheme.

5.1 Off-line estimation of machine inductances

An appropriate method is important in the estimation of electric machine parameters. The finite-element method (FEM) is a very powerful tool in the estimation of machine parameters, since it takes into account the geometry details, the actual distribution of windings, and the nonlinearity of magnetic materials (Chang, 1996). The 2-D FEM can provide acceptable results although some geometry details are inherently omitted (such as end windings). The problem with the FEM is the calculation time, which is the longer the finer mesh is used (Dajaku and Gerling, 2010a). Moreover, in some cases the 2-D FEM is insufficient, and thus, the 3-D FEM is needed, which is more difficult to construct and requires more elements.

In this thesis, the off-line parameter estimation is specified as a procedure to obtain machine parameters from FEM models or by controlling the actual machine in different load conditions

required by the estimation scheme. The off-line estimation of machine parameters can also be performed by a separate voltage supply. Such a technique is, for example, an AC standstill test (Dutta and Rahman, 2006).

5.1.1 Publication III – Off-line methods

Publication III studies three off-line methods to determine the decoupled D–Q model inductance parameters. The inductances are determined using the 2-D FEM of ANSYS Maxwell and the 2-D FEM including skewing of Flux 2D by CEDRAT. In addition, an experimental determination is performed by supplying the machine by VSIs.

The first studied method in Publication III uses the phase-variable inductance waveforms obtained from the 2-D FEA. The waveforms are then transformed with the proposed transformation (4.4). The method originates from the model derivation, and is therefore straightforward to apply, but requires the knowledge of the inductances in different rotor positions. Thus, it is important that the rotor angle θ is known precisely, and that the phase sequence is correct.

The second method uses flux-current relations. In that method, the FEM model is supplied with a specific current aligned with the desired axis. The method applies the fundamental definition of inductances and thereby valid values are expected. The rotor position must be known precisely also with this method in order to supply the current with the desired reference frame axis. In principle, this method should provide same values as the previous method, but because of the differences in the calculation of fluxes and inductances of the used FEM software, there are some discrepancies, as shown in Publication III.

The third method studied uses the stator voltage equations of the decoupled D–Q model. In this method, the machine is supplied by VSIs. The inductance parameters are then calculated from the reference voltages, the measured currents, and the electrical rotational speed. Because, in addition to the inductances, the stator voltage equations include the stator resistance and the PM flux, two adjacent operating points are considered. This eliminates their effect on the inductance calculation. The experimental results of Publication III show that the method provides inductance values with an acceptable agreement compared with the corresponding FEA values. In addition, the parameters obtained with the VSI supply were validated by tuning model-based current controllers. Thus, the method is applicable to the determination of the inductances of actual machines supplied by VSIs.

5.1.2 AC standstill test

The AC standstill test was applied to this particular double-star IPM machine to have experimental values with which the results obtained by the VSI-supply method in Publication III can be compared. In the AC standstill test one phase is supplied with an AC voltage source while the other windings are open circuited. The voltages induced in the open windings are measured in different rotor positions. Figure 5.1 shows the measurement arrangement. The advantage of the method is that the current, the induced voltages, and the rotor position can be measured accurately. The generated load condition, however, does not correspond with the normal operating point of the

machine. Moreover, the effect of saturation is not fully considered in the way it can be considered with the VSI supply.

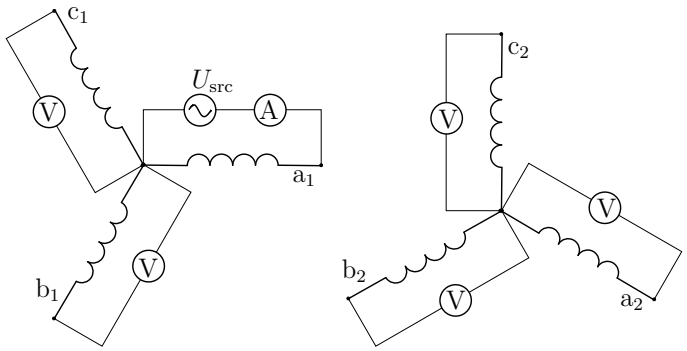

(a) winding set 1 (b) winding set 2

Figure 5.1: Supply arrangement to measure phase-variable inductances in different rotor positions. The phase a_1 is supplied by an AC voltage source, 10 V and 50 Hz. The symbols V and A represent the voltage and current measurements, respectively.

The phase a_1 was selected as the reference winding and it was supplied by an AC voltage source of 10 V and 50 Hz. The phase current in the winding and the induced voltages in the other windings were measured with a Yokogawa Power Analyzer. The rotor electrical angle was varied from zero to 180 degrees with 9-degree increments. The rotor position was measured with an incremental encoder attached to a dSPACE system. Figure 5.2 shows the measured inductance waveforms and the corresponding approximate waveforms that include only the second harmonic. Although the measured inductance waveforms cannot be represented perfectly with fundamental components only, a satisfactory agreement can be observed.

Table 5.1 lists the inductance parameters in the decoupled D–Q reference frames. The methods

Table 5.1: Calculated inductance parameters using the coefficients from the waveforms of Figure 5.2 obtained by the AC standstill test. The values from Publication III obtained with the VSI supply are shown for comparison.

Inductance	AC standstill test	VSI supply
L_{D_1}	34.0 [mH]	35.6 [mH]
L_{Q_1}	55.1 [mH]	57.3 [mH]
L_{D_2}	8.8 [mH]	7.8 [mH]
L_{Q_2}	11.7 [mH]	12.7 [mH]

provide similar values, and are thus applicable to double-star IPM machines.

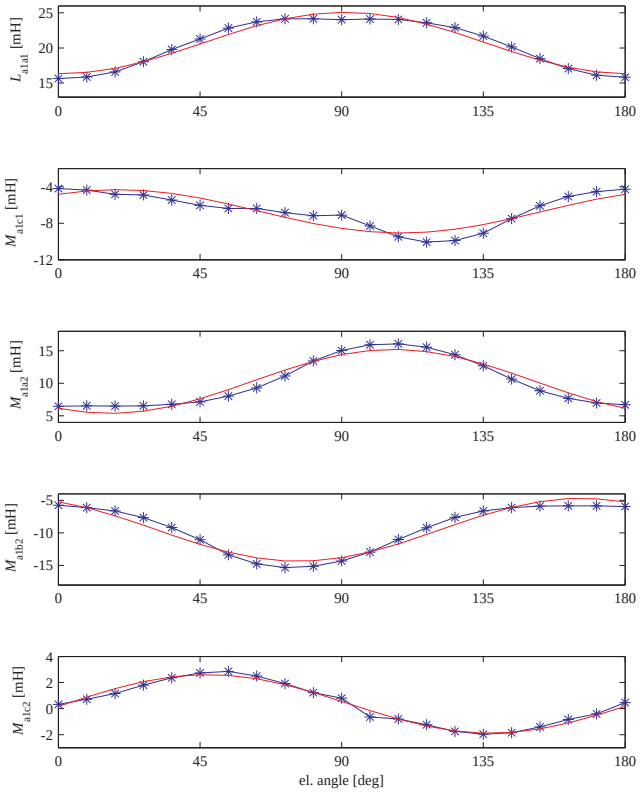

Figure 5.2: Phase-variable inductance waveforms for the phase a_1. From top to bottom: the self-inductance L_{a1a1}, the mutual inductance between the phases a_1 and c_1 (phases of the same star) M_{a1c1}, and the mutual inductances between the phases a_1–a_2, a_1–b_2, and a_1–c_2 (phases of different stars) M_{a1a2}, M_{a1b2}, and M_{a1c2}, respectively. The blue curves with stars are the measured values whereas the red curves correspond to the approximate waveforms that include only the second harmonic.

5.2 On-line parameter estimation

On-line estimation of machine parameters provides benefits in many applications such as model-based control methods. In this thesis, the on-line parameter estimation is specified as an operating state estimation applying only the signals used for the machine control. Standstill is considered a special case of on-line estimation. At a standstill, appropriate excitation signals are needed.

5.2.1 Publication IV – RLS method

Publication IV proposes an RLS-based on-line estimator for double-star PM machines. The estimation can be carried out at a standstill and in a rotating operating state. Only the measurements used for the machine control are needed.

In the standstill estimation, suitable voltages are supplied at the machine terminals by VSIs that are used to control the machine. The rotor is assumed not to be locked, and thus, the resulting currents must maintain the machine at a standstill. This requirement is easily met in the D_2–Q_2 reference frame since these current components do not interact with the flux produced by the PMs, and therefore, no torque is produced. Thus, the value for the stator resistance can be easily identified at a standstill by using the D_2–Q_2 reference frame. Inductances, instead, must be estimated on the axis in question.

The estimation in the rotating operating state is based on the voltage and current models of the double-star PM machine. The voltage model, in which the only unknown model parameter in the calculation is the stator resistance, is first used to calculate the stator flux linkage. Since typically only the currents are measured and not the voltages, there are differences between the estimated and actual terminal voltages. The voltage error caused by the converter nonlinearity can be mitigated by applying the techniques proposed in (Munoz and Lipo, 1999; Liu et al., 2012), estimated as in (Morimoto et al., 2006; Inoue et al., 2009) or considered as an acceptable error as is done here. The effect of the voltage error is more significant at low speeds, especially in the estimation of the PM flux.

5.3 Conclusion

The parameters of the double-star IPM machine were determined both off-line and on-line. The off-line methods comprise phase-variable inductance waveforms, flux-current relations, and stator voltage equations in the decoupled D–Q reference frames. The methods were evaluated by a 2-D FEM, and experimental results were provided by applying the stator-voltage-equation-based method. All the methods discussed in Publication III can be used in different load conditions, and thus, the saturation can be taken into account. Although the methods yield similar values, some discrepancies can also be observed.

The phase-variable inductance waveforms were also measured by an AC standstill test using a one-phase voltage supply. The obtained values are in a good agreement with the experimental values obtained by the stator-voltage-equation-based method. The method, however, requires a special supply arrangement, and thus, the VSI supply provides a more feasible solution.

An on-line estimation method based on the RLS algorithm and the machine model was also evaluated. The method is well established and simple to implement. In the literature, the method has been used for the parameter estimation of three-phase machines. The results show that the method is valid also for double-star IPM machines. With this method, the inductance parameters and the PM flux can be updated in different load conditions. As a drawback the method is not applicable to the estimation of the PM flux at low speeds in the considered case because of the voltage error between the reference voltage and actual terminal voltage.

Chapter 6

Conclusions and further study

In this doctoral thesis, a D–Q model for double-star permanent-magnet synchronous machines (PMSMs) was derived and methods to determine the model parameters were proposed. The stator of the studied double-star PMSM consists of two three-phase winding sets with separated neutral points. The displacement between the sets is considered as a parameter. The rotor includes PMs that are buried in the rotor core, thus representing a salient-pole structure in which the inductances depend on the rotor position. The studied machine is referred to as double-star interior-permanent-magnet (IPM) machine.

The derived D–Q model consists of two D–Q reference frames that are decoupled; capital DQ letters are used to distinguish the decoupled D–Q reference frames from the three-phase d–q reference frame. The model was derived with a transformation that was obtained by finding a matrix that diagonalizes the stator inductance matrix and eliminates the rotor position dependence of inductances (only the fundamental components of the phase-variable inductances were considered). Diagonalization reduces the number of parameters, yet retains the characteristic properties of the initial matrix and results in the simplest possible form of the system. The derived transformation has a specific feature that is similar to the existing vector-space decomposition transformation: when the displacement between the sets is 30°, the fundamental component and the harmonics of the order 11, 13, 23, 25, etc. are mapped into one reference frame and the harmonics of the order 5, 7, 17, 19, etc. are mapped into another reference frame. The mapping of harmonics depends on the displacement between the sets.

The parameters of the double-star IPM machine were determined both off-line and on-line. The off-line methods comprise phase-variable inductance waveforms, flux-current relations, and stator voltage equations in the decoupled D–Q reference frames. The methods were evaluated by a 2-D FEM, and experimental results were provided applying the stator-voltage-equation-based method. All the methods can be used in different load conditions, and thus, the saturation can be taken into account. Although the methods yield similar values, some discrepancies can also be observed. The well-established RLS method for on-line estimation of three-phase machine parameters was extended to double-star IPM machines. The method is well established and simple to implement. With this method, the inductance parameters and the PM flux can be updated in different load conditions. As a drawback, the method is not applicable to the estimation of the PM flux at low speeds in this particular machine drive, unless the voltage error is compensated.

The derived decoupled D–Q model has been demonstrated to be effective with an example double-star IPM machine, in which the displacement between the sets is 30 electrical degrees. The two sets displaced by 30° provide enhanced torque characteristics when compared with conventional three-phase machines. The accuracy of the model is improved by taking into account the rotor-based harmonics, namely the harmonics in the no-load flux linkage. The obtained accuracy improvement depends highly on the magnet magnetization and the rotor geometry. When also taking into account the rotor-based harmonics, the model becomes more complex.

The decoupled D–Q model of double-star PMSMs derived in this doctoral thesis is suitable for model-based control design as well as for general analysis of double-star PM machines. The proposed transformation simplifies the machine model by eliminating the mutual coupling of the fundamental components and by representing the variables in reference frames where the inductances do not depend on the rotor position.

6.1 Suggestions for future work

As the main motivation for the modeling of double-star IPM machines was the model-based control design, it is of interest to study different control methods and especially, to optimize the transient behavior of the drive system.

It would be advisable to extend the modeling concept to m-star machines because the torque quality can be further improved by increasing the number of winding sets. Moreover, by increasing the number of winding sets, also the redundancy of the system can be increased. Redundancy is a desirable feature because it is increasingly important to guarantee uninterrupted operation of various electric drive systems also under fault conditions. Especially in safety-critical applications the continuous operation is of paramount importance. Therefore, it would be worth studying how the model has to be modified for fault tolerant control of double-star PM machines.

Finally, the on-line estimation of machine parameters could be considered with the MRAS-based estimator and investigate if multiple parameters could be estimated simultaneously in the case of double-star PM machines.

Bibliography

Abbas, M.A., Christen, R., and Jahns, T.M. (1984), "Six-Phase Voltage Source Inverter Driven Induction Motor," *IEEE Transactions on Industry Applications*, vol. IA-20, no. 5, pp. 1251–1259.

Andriollo, M., Bettanini, G., Martinelli, G., Morini, A., and Tortella, A. (2009), "Analysis of Double-Star Permanent-Magnet Synchronous Generators by a General Decoupled *d–q* Model," *IEEE Transactions on Industry Applications*, vol. 45, no. 4, pp. 1416–1424.

Ban, D., Zarko, D., and Mandic, I. (2005), "Turbogenerator End-Winding Leakage Inductance Calculation Using a 3-D Analytical Approach Based on the Solution of Neumann Integrals," *IEEE Transactions on Energy Conversion*, vol. 20, no. 1, pp. 98–105.

Barcaro, M., Bianchi, N., and Magnussen, F. (2010), "Analysis and Tests of a Dual Three-Phase 12-Slot 10-Pole Permanent-Magnet Motor," *IEEE Transactions on Industry Applications*, vol. 46, no. 6, pp. 2355–2362.

Bechouche, A., Sediki, H., Ould Abdeslam, D., and Haddad, S. (2012), "A Novel Method for Identifying Parameters of Induction Motors at Standstill Using ADALINE," *IEEE Transactions on Energy Conversion*, vol. 27, no. 1, pp. 105–116.

Bianchi, N. (2002), *Electrical Machine Analysis Using Finite Elements*, Boca Raton: CRC Press.

Blaabjerg, F., Liserre, M., and Ma, K. (2012), "Power Electronics Converters for Wind Turbine Systems," *IEEE Transactions on Industry Applications*, vol. 48, no. 2, pp. 708–719.

Blaabjerg, F. and Ma, K. (2013), "Future on Power Electronics for Wind Turbine Systems," *IEEE Journal of Emerging and Selected Topics in Power Electronics*, vol. 1, no. 3, pp. 139–152.

Boglietti, A., Bojoi, R., Cavagnino, A., and Tenconi, A. (2008), "Efficiency Analysis of PWM Inverter Fed Three-Phase and Dual Three-Phase High Frequency Induction Machines for Low/Medium Power Applications," *IEEE Transactions on Industrial Electronics*, vol. 55, no. 5, pp. 2015–2023.

Boileau, T., Leboeuf, N., Nahid-mobarakeh, B., and Meibody-Tabar, F. (2011), "Online Identification of PMSM Parameters: Parameter Identifiability and Estimator Comparative Study," *IEEE Transactions on Industry Applications*, vol. 47, no. 4, pp. 1944–1957.

Bojoi, R., Lazzari, M., Profumo, F., and Tenconi, A. (2003), "Digital Field-Oriented Control for Dual Three-Phase Induction Motor Drives," *IEEE Transactions on Industry Applications*, vol. 39, no. 3, pp. 752–760.

Bojoi, R., Levi, E., Farina, F., Tenconi, A., and Profumo, F. (2006), "Dual three-phase induction motor drive with digital current control in the stationary reference frame," *IET Electric Power Applications*, vol. 153, no. 1, pp. 129–139.

Briz, F., Degner, M.W., and Lorenz, R.D. (2000), "Analysis and Design of Current Regulators Using Complex Vectors," *IEEE Transactions on Industry Applications*, vol. 36, no. 3, pp. 817–825.

Chang, L. (1996), "An Improved FE Inductance Calculation for Electrical Machines," *IEEE Transactions on Magnetics*, vol. 32, no. 4, pp. 3237–3245.

Che, H.S., Hew, W.P., Rahim, N.A., Levi, E., Jones, M., and Duran, M.J. (2012), "Current Control of a Six-Phase Induction Generator for Wind Energy Plants," in *Proc. 15th Int. Power Electronics and Motion Control Conf. EPE-PEMC ECCE Europe*.

Che, H.S., Levi, E., Jones, M., Duran, M.J., Hew, W.P., and Rahim, N.A. (2014), "Operation of a Six-Phase Induction Machine Using Series-Connected Machine-Side Converters," *IEEE Transactions on Industrial Electronics*, vol. 61, no. 1, pp. 164–176.

Clarke, E. (1943), *Circuit Analysis of A-C Power Systems*, vol. I, New York: John Wiley & Sons.

Dajaku, G. and Gerling, D. (2010a), "Determination of Air-Gap Flux Density due to Magnets using the New Analytical Model," in *Proc. XIX Int. Electrical Machines Conf. ICEM*, pp. 1–6, Rome, Italy.

Dajaku, G. and Gerling, D. (2010b), "Stator Slotting Effect on the Magnetic Field Distribution of Salient Pole Synchronous Permanent-Magnet Machines," *IEEE Transactions on Magnetics*, vol. 46, no. 9, pp. 3676–3683.

Duran, M.J., Kouro, S., Wu, B., Levi, E., Barrero, F., and Alepuz, S. (2011), "Six-phase PMSG wind energy conversion system based on medium-voltage multilevel converter," in *Proc. 14th Power Electron. and Appl. European Conf. EPE ECCE Europe*, pp. 1–10, Birmingham, UK.

Dutta, R. and Rahman, M.F. (2006), "A Comparative Analysis of Two Test Methods of Measuring *d*- and *q*-Axes Inductances of Interior Permanent-Magnet Machine," *IEEE Transactions on Magnetics*, vol. 42, no. 11, pp. 3712–3718.

EEA (2012), "Renewable energy production must grow fast to reach the 2020 target," European Environment Agency, URL http://www.eea.europa.eu/highlights/renewable-energy-production-must-grow, accessed June 30th, 2013.

EWEA (2013), "Wind energy facts," The European Wind Energy Association, URL http://www.ewea.org/fileadmin/files/library/publications/statistics/Factsheets.pdf, accessed December 18th, 2013.

Figueroa, J., Cros, J., and Viarouge, P. (2006), "Generalized Transformations for Polyphase Phase-Modulation Motors," *IEEE Transactions on Energy Conversion*, vol. 21, no. 2, pp. 332–341.

Fortescue, C.L. (1918), "Method of Symmetrical Co-Ordinates Applied to the Solution of Polyphase Networks," *Transactions of the American Institute of Electrical Engineers*, vol. XXXVII, no. 2, pp. 1027–1140.

Fuchs, E. and Rosenberg, L. (1974), "Analysis of an Alternator with Two Displaced Stator Windings," *IEEE Transactions on Power Apparatus and Systems*, vol. PAS-93, no. 6, pp. 1776–1786.

Hadiouche, D., Razik, H., and Rezzoug, A. (2000), "Study and simulation of space vector PWM control of double-star induction motors," in *Proc. VII IEEE Int. Power Electron. Congress CIEP*, pp. 42–47.

Hadiouche, D., Razik, H., and Rezzoug, A. (2004), "On the Modelling and Design of Dual-Stator Windings to Minimize Circulating Harmonic Currents for VSI Fed AC Machines," *IEEE Transactions on Industry Applications*, vol. 40, no. 2, pp. 506–515.

Hamida, M.A., Leon, J.D., Glumineau, A., and Boisliveau, R. (2013), "An Adaptive Interconnected Observer for Sensorless Control of PM Synchronous Motors With Online Parameter Identification," *IEEE Transactions on Industrial Electronics*, vol. 60, no. 2, pp. 739–748.

Hansen, L.H., Madsen, P.H., Blaabjerg, F., Christensen, H.C., Lindhard, U., and Eskildsen, K. (2001), "Generators and Power Electronics Technology for Wind Turbines," in *Proc. 27th Annu. IEEE Ind. Electron. Society Conf. IECON*, vol. 3, pp. 2000–2005.

Heikkilä, T. (2002), *Permanent Magnet Synchronous Motor for Industrial Inverter Applications – Analysis and Design*, Doctoral thesis, Acta Universitatis Lappeenrantaensis 134, Lappeenranta University of Technology, Finland.

Hsieh, M.F., Hsu, Y.C., Dorrell, D.G., and Hu, K.H. (2007), "Investigation on End Winding Inductance in Motor Stator Windings," *IEEE Transactions on Magnetics*, vol. 43, no. 6, pp. 2513–2515.

Huh, K.K. (2008), *Discrete-Time Modeling, Control and Signal Processing for AC Drives and Motion Servo System Diagnostics*, Ph.D. thesis, University of Wisconsin–Madison, United States.

Ichikawa, S., Tomita, M., Doki, S., and Okuma, S. (2006), "Sensorless Control of Permanent-Magnet Synchronous Motors Using Online Parameter Identification Based on System Identification Theory," *IEEE Transactions on Industrial Electronics*, vol. 53, no. 2, pp. 363–372.

Inoue, Y., Morimoto, S., and Sanada, M. (2009), "Control Method for Direct Torque Controlled PMSG in Wind Power Generation System," in *Proc. Int. IEEE Electric Machines and Drives Conf. IEMDC*, pp. 1231–1238.

Inoue, Y., Kawaguchi, Y., Morimoto, S., and Sanada, M. (2011), "Performance Improvement of Sensorless IPMSM Drives in a Low-Speed Region Using Online Parameter Identification," *IEEE Transactions on Industry Applications*, vol. 47, pp. 798–804.

Jahns, T.M. (1980), "Improved Reliability in Solid-State AC Drives by Means of Multiple Independent Phase Drive Units," *IEEE Transactions on Industry Applications*, vol. IA-16, no. 3, pp. 321–331.

Jahns, T.M. and Soong, W.L. (1996), "Pulsating Torque Minimization Techniques for Permanent Magnet AC Motor Drives – A Review," *IEEE Transactions on Industrial Electronics*, vol. 43, no. 2, pp. 321–330.

Kallio, S., Andriollo, M., Tortella, A., and Karttunen, J. (2013), "Decoupled d-q Model of Double-Star Interior Permanent Magnet Synchronous Machines," *IEEE Transactions on Industrial Electronics*, vol. 60, no. 6, pp. 2486–2494.

Kanerva, S., Toivanen, O., Sario, P., and Arshad, W. (2008), "Experimental Study on Harmonic Losses of a Dual-Stator Synchronous Motor with Redundant Voltage Source Inverter (VSI) Drive," in *Proc. 18th Int. Electrical Machines Conf. ICEM*, pp. 1–4.

Kataoka, T., Watanabe, E.H., and Kitano, J. (1981), "Dynamic Control of a Current-Source Inverter/Double-Wound Synchronous Machine System for AC Power Supply," *IEEE Transactions on Industry Applications*, vol. IA-17, no. 3, pp. 314–320.

Knudsen, A. (1995), "Extended Park's Transformation for 2x3-phase Synchronous Machine and Converter Phasor Model with Representation of AC Harmonics," *IEEE Transactions on Energy Conversion*, vol. 10, no. 1, pp. 126–132.

Krause, P.C., Wasynczuk, O., and Sudhoff, S.D. (2002), *Analysis of Electric Machinery and Drive Systems, Second Edition*, New York: John Wiley & Sons.

Levi, E. (2008), "Multiphase Electric Machines for Variable-Speed Applications," *IEEE Transactions on Industrial Electronics*, vol. 55, no. 5, pp. 1893–1909.

Levi, E., Bojoi, R., Profumo, F., Toliyat, H.A., and Williamson, S. (2007), "Multiphase induction motor drices – a technology status review," *IET Electric Power Applications*, vol. 1, no. 4, pp. 489–516.

Levi, E., Jones, M., Vukosavic, S.N., and Toliyat, H.A. (2004), "A Novel Concept of a Multiphase, Multimotor Vector Controlled Drive System Supplied From a Single Voltage Source Inverter," *IEEE Transactions on Power Electronics*, vol. 19, no. 2, pp. 320–335.

Lipo, T.A. (1980), "A d-q Model for Six Phase Induction Machines," in *Proc. Int. Electrical Machines Conf. ICEM*, pp. 860–867.

Lipo, T.A. (2012), *Analysis of Synchronous Machines*, Boca Raton: CRC Press, second edn.

Liserre, M., Cardenas, R., Molinas, M., and Rodriguez, J. (2011), "Overview of Multi-MW Wind Turbines and Wind Parks," *IEEE Transactions on Industrial Electronics*, vol. 58, no. 4, pp. 1081–1095.

Liu, K., Zhang, Q., Chen, J., Z.Q.Zhu, and Zhang, J. (2011), "Online Multiparameter Estimation of Nonsalient-Pole PM Synchronous Machines With Temperature Variation Tracking," *IEEE Transactions on Industrial Electronics*, vol. 58, no. 5, pp. 1776–1788.

Liu, K., Zhu, Z.Q., Zhang, Q., and Zhang, J. (2012), "Influence of Nonideal Voltage Measurement on Parameter Estimation in Permanent-Magnet Synchronous Machines," *IEEE Transactions on Industrial Electronics*, vol. 59, no. 6, pp. 2438–2447.

Miller, T.J.E. and McGilp, M.I. (2009), "Analysis of Multi-Phase Permanent-Magnet Synchronous Machines," in *Proc. Int. Electrical Machines and Systems Conf. ICEMS*, pp. 1–6.

Mohammed, O., Liu, S., and Liu, Z. (2004), "Phase-variable model of PM synchronous machines for integrated motor drives," *IET Science, Measurement Technology*, vol. 151, no. 6, pp. 423–429.

Mohammed, O., Liu, S., and Liu, Z. (2007), "FE-based physical phase variable model of PM synchronous machines under stator winding short circuit faults," *IET Science, Measurement Technology*, vol. 1, no. 1, pp. 12–16.

Morimoto, S., Sanada, M., and Takeda, Y. (2006), "Mechanical Sensorless Drives of IPMSM With Online Parameter Identification," *IEEE Transactions on Industry Applications*, vol. 42, no. 5, pp. 1241–1248.

Munoz, A.R. and Lipo, T.A. (1999), "On-Line Dead-Time Compensation Technique for Open-Loop PWM–VSI Drives," *IEEE Transactions on Power Electronics*, vol. 14, no. 4, pp. 683–689.

Nelson, R.H. and Krause, P.C. (1974), "Induction Machine Analysis for Arbitrary Displacement Between Multiple Winding Sets," *IEEE Transactions on Power Apparatus and Systems*, vol. PAS-93, no. 3, pp. 841–848.

Obe, E.S. (2009), "Direct computation of ac machine inductances based on winding function theory," *Energy Conversion and Management*, vol. 50, pp. 539–542.

Park, R.H. (1929), "Two-Reaction Theory of Synchronous Machines: Generalized Methods of Analysis - Part I," *Transactions of the American Institute of Electrical Engineers*, vol. 48, no. 3, pp. 716–727.

Parsa, L. (2005), "On Advantages of Multi-Phase Machines," in *Proc. 31st IEEE Ind. Electron. Society Annu. Conf. IECON*, p. 6.

Peretti, L. and Zigliotto, M. (2012), "Automatic procedure for induction motor parameter estimation at standstill," *IET Electric Power Applications*, vol. 6, no. 4, pp. 214–224.

Riveros, J.A., Yepes, A.G., Barrero, F., Doval-Gandoy, J., Bogado, B., Lopez, O., Jones, M., and Levi, E. (2012), "Parameter Identification of Multiphase Induction Machines With Distributed Windings — Part 2: Time-Domain Techniques," *IEEE Transactions on Energy Conversion*, vol. 27, no. 4, pp. 1067–1077.

Schiferl, R.F. and Ong, C.M. (1983a), "Six Phase Synchronous Machine With AC and DC Stator Connections, Part I: Equivalent Circuit Representation and Steady-State Analysis," *IEEE Transactions on Power Apparatus and Systems*, vol. PAS-102, no. 8, pp. 2685–2693.

Schiferl, R. and Ong, C. (1983b), "Six Phase Synchronous Machine With AC and DC Stator Connections, Part II: Harmonic Studies and a Proposed Uninterruptible Power Supply Scheme," *IEEE Transactions on Power Apparatus and Systems*, vol. PAS-102, no. 8, pp. 2694–2701.

Shi, Y., Sun, K., Huang, L., and Li, Y. (2012), "Online Identification of Permanent Magnet Flux Based on Extended Kalman Filter for IPMSM Drive With Position Sensorless Control," *IEEE Transactions on Industrial Electronics*, vol. 59, no. 11, pp. 4169–4178.

Simoes, M.G. and Vieira, P.J. (2002), "A High-Torque Low-Speed Multiphase Brushless Machine – A Perspective Application for Electric Vehicles," *IEEE Transactions on Industrial Electronics*, vol. 49, no. 5, pp. 1154–1164.

Tang, K.T. (2007), *Mathematical Methods for Engineers and Scientists 1: Complex Analysis, Determinants and Matrices*, Berlin: Springer-Verlag.

Tessarolo, A. (2010), "Analysis of Split-Phase Electric Machines with Unequally-Loaded Stator Windings and Distorted Phase Currents," in *Proc. XIX Int. Electrical Machines Conf. ICEM*, pp. 1–7, Rome, Italy.

Tessarolo, A. and Luise, F. (2008), "An Analytical-Numeric Method for Stator End-Coil Leakage Inductance Computation in Multi-Phase Electric Machines," in *Proc. IEEE Ind. Appl. Society Annu. Meeting IAS*, pp. 1–8.

UpWind (2011), "Design Limits and Solution for Very Large Wind Turbines," Tech. rep., UpWind project, URL http://www.ewea.org/fileadmin/ewea_documents/documents/upwind/21895_UpWind_Report_low_web.pdf.

Valverde, G., Kyriakides, E., Heydt, G.T., and Terzija, V. (2011), "Nonlinear Estimation of Synchronous Machine Parameters Using Operating Data," *IEEE Transactions on Energy Conversion*, vol. 26, no. 3, pp. 831–839.

Vas, P. (1998), *Sensorless Vector And Direct Torque Control*, Oxford: Oxford University Press.

WWEA (2012), "2012 Annual Report," The World Wind Energy Association, URL http://www.wwindea.org/webimages/WorldWindEnergyReport2012_final.pdf, accessed December 17th, 2013.

Yepes, A.G., Riveros, J.A., Doval-Gandoy, J., Barrero, F., Lopez, O., Bogado, B., Jones, M., and Levi, E. (2012), "Parameter Identification of Multiphase Induction Machines With Distributed Windings – Part 1: Sinusoidal Excitation Methods," *IEEE Transactions on Energy Conversion*, vol. 27, no. 4, pp. 1056–1066.

Zhao, Y. and Lipo, T. (1995), "Space Vector PWM Control of Dual Three-Phase Induction Machine Using Vector Space Decomposition," *IEEE Transactions on Industry Applications*, vol. 31, no. 5, pp. 1100–1109.

Zubia, I., Zatarain, A., Alcalde, C., and Ostolaza, X. (2011), "In situ electrical parameter identification method for induction wind generators," *IET Electric Power Applications*, vol. 5, no. 7, pp. 549–557.

Appendix A

Experimental machine data

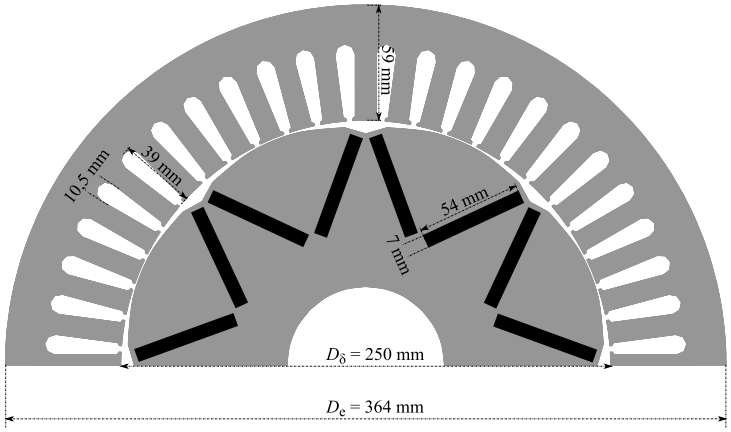

Geometrical dimensions of the stator and the rotor of the double-star IPM synchronous machine.

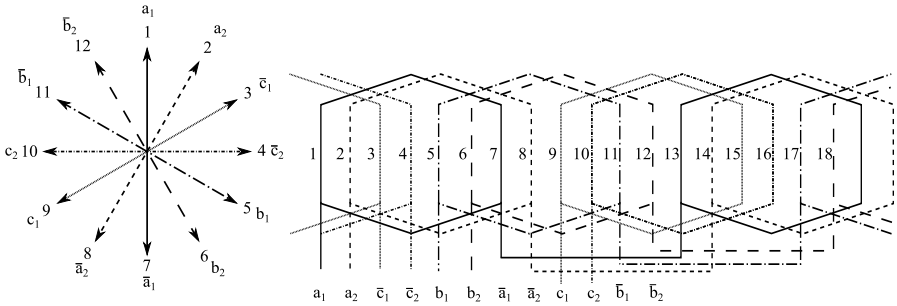

Double-star winding system: the base winding star and the winding layout. The phase coil groups are connected in series.

Table A.1: Parameters of the double-star IPM synchronous machine.

Description	Unit	Value
Nominal power, P_n	kW	25
Nominal current, I_n	A	22.5
Nominal voltage, U_n	V	380
Nominal frequency, f_n	Hz	23.3
Number of poles, $2p$		8
Stator resistance, R_s	mΩ	530
d-axis magnetizing inductance, L_md	mH	22.0
q-axis magnetizing inductance, L_md	mH	29.5
Leakage inductance, L_σ	mH	4.5
Frame size		225
Outer diameter, D_e	mm	364
Air-gap diameter, D_δ	mm	250
Stack length, l	mm	270
Air-gap minimum length, δ_0	mm	1.2
Phases, n		6
Stator slots, Q_s		48
Slot cross-sectional area	mm^2	240
Insulated slot area	mm^2	215
Copper fill factor		0.6
Number of slots per pole and phase, q		1
Winding type		full-pitch winding
Winding step		1–7
Winding factors	k_w1	0.989
	k_w5	0.738
	k_w7	0.527
	k_w11	0.090
	k_w13	0.076
Diameters of wires in parallel	mm	1.12 mm × 3
	mm	0.9 mm × 2
Winding turns in series per stator phase		120
Conductors per slot		30
Number of coil groups		24
Parallel paths		1
Current density at nominal torque	$\mathrm{A/mm}^2$	5.3

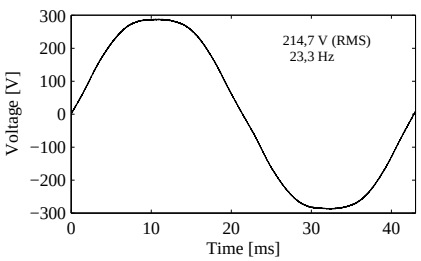

(a) Back EMF (phase-to-neutral).

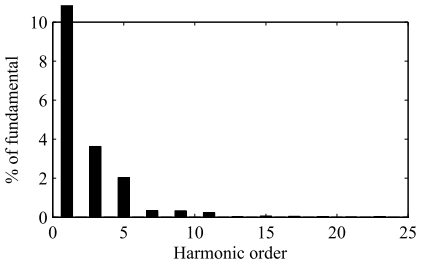

(b) Spectrum.

Measured back EMF (phase-to-neutral) and its harmonic content at the nominal speed 350 r/min.

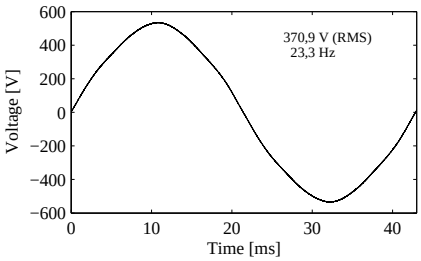

(c) Back EMF (phase-to-phase).

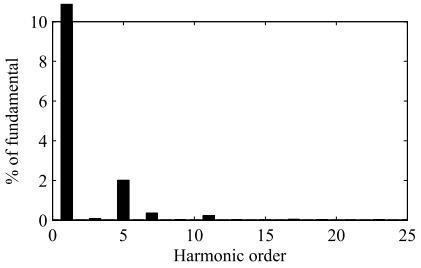

(d) Spectrum.

Measured back EMF (phase-to-phase) and its harmonic content at the nominal speed 350 r/min.

ACTA UNIVERSITATIS LAPPEENRANTAENSIS

529. LAISI, MILLA. Deregulation's impact on the railway freight transport sector's future in the Baltic Sea region. 2013. Diss.

530. VORONIN, SERGEY. Price spike forecasting in a competitive day-ahead energy market. 2013. Diss.

531. PONOMAREV, PAVEL. Tooth-coil permanent magnet synchronous machine design for special applications. 2013. Diss.

532. HIETANEN, TOMI. Magnesium hydroxide-based peroxide bleaching of high-brightness mechanical pulps. 2013. Diss.

533. TYKKÄLÄ, TOMMI M. Real-time image-based RGB-D camera motion tracking and environment mapping. 2013. Diss.

534. PEKKOLA, SANNA. Performance measurement and management in a collaborative network. 2013. Diss.

535. PANOREL, IRIS CHERRY. Pulsed corona discharge as an advanced oxidation process for the degradation of organic compounds in water. 2013. Diss.

536. TORKKELI, LASSE. The influence of network competence of internationalization of SMEs. 2013. Diss.

537. MOLANDER, SOLE. Productivity and services – safety telephone services for the elderly. 2013. Diss.

538. SITARZ, ROBERT. Identification of research trends in the field of separation processes. Application of epidemiological model, citation analysis, text mining, and technical analysis of the financial markets. 2013. Diss.

539. KATTEDEN, KAMIEV. Design and testing of an armature-reaction-compensated permanent magnet synchronous generator for island operation. 2013. Diss.

540. HÄMÄLÄINEN, HARRI. Integration of learning supportive applications to development of e-portfolio construction process. 2013. Diss.

541. RATCHANANUSORN, WARIN. Development of a process for the direct synthesis of hydrogen peroxide in a novel microstructured reactor. 2013. Diss.

542. PERFILEV, DANIIL. Methodology for wind turbine blade geometry optimization. 2013. Diss.

543. STROKINA, NATALIYA. Machine vision methods for process measurements in pulping. 2013. Diss.

544. MARTTONEN, SALLA. Modelling flexible asset management in industrial maintenance companies and networks. 2013. Diss.

545. HAKKARAINEN, JANNE. On state and parameter estimation in chaotic systems. 2013. Diss.

546. HYYPIÄ, MIRVA. Roles of leadership in complex environments
Enhancing knowledge flows in organisational constellations through practice-based innovation processes. 2013. Diss.

547. HAAKANA, JUHA. Impact of reliability of supply on long-term development approaches to electricity distribution networks. 2013. Diss.

548. TUOMINEN, TERHI. Accumulation of financial and social capital as means to achieve a sustained competitive advantage of consumer co-operatives. 2013. Diss.

549. VOLCHEK, DARIA. Internationalization of small and medium-sized enterprises and impact of institutions on international entrepreneurship in emerging economies: the case of Russia. 2013. Diss.

550. PEKKARINEN, OLLI. Industrial solution business – transition from product to solution offering. 2013. Diss.

551. KINNUNEN, JYRI. Risk-return trade-off and autocorrelation. 2013. Diss.

552. YLÄTALO, JAAKKO. Model based analysis of the post-combustion calcium looping process for carbon dioxide capture. 2013. Diss.

553. LEHTOVAARA, MATTI. Commercialization of modern renewable energy. 2013. Diss.

554. VIROLAINEN, SAMI. Hydrometallurgical recovery of valuable metals from secondary raw materials. 2013. Diss.

555. HEINONEN, JARI. Chromatographic recovery of chemicals from acidic biomass hydrolysates. 2013. Diss.

556. HELLSTÉN, SANNA. Recovery of biomass-derived valuable compounds using chromatographic and membrane separations. 2013. Diss.

557. PINOMAA, ANTTI. Power-line-communication-based data transmission concept for an LVDC electricity distribution network – analysis and implementation. 2013. Diss.

558. TAMMINEN, JUSSI. Variable speed drive in fan system monitoring. 2013. Diss.

559. GRÖNMAN, KAISA. Importance of considering food waste in the development of sustainable food packaging systems. 2013. Diss.

560. HOLOPAINEN, SANNA. Ion mobility spectrometry in liquid analysis. 2013. Diss.

561. NISULA, ANNA-MAIJA. Building organizational creativity – a multitheory and multilevel approach for understanding and stimulating organizational creativity. 2013. Diss.

562. HAMAGUCHI, MARCELO. Additional revenue opportunities in pulp mills and their impacts on the kraft process. 2013. Diss.

563. MARTIKKA, OSSI. Impact of mineral fillers on the properties of extruded wood-polypropylene composites. 2013. Diss.

564. AUVINEN, SAMI. Computational modeling of the properties of TiO2 nanoparticles. 2013. Diss.

565. RAHIALA, SIRPA. Particle model for simulating limestone reactions in novel fluidised bed energy applications. 2013. Diss.

566. VIHOLAINEN, JUHA. Energy-efficient control strategies for variable speed controlled parallel pumping systems based on pump operation point monitoring with frequency converters. 2014. Diss.

567. VÄISÄNEN, SANNI. Greenhouse gas emissions from peat and biomass-derived fuels, electricity and heat – Estimation of various production chains by using LCA methodology. 2014. Diss.

568. SEMYONOV, DENIS. Computational studies for the design of process equipment with complex geometries. 2014. Diss.

569. KARPPINEN, HENRI. Reframing the relationship between service design and operations: a service engineering approach. 2014. Diss.